Remote Sensing of Environment 286 (2023) 113441

Contents lists available at ScienceDirect

Remote Sensing of Environment

journal homepage: www.elsevier.com/locate/rse

Assessing the resilience of ecosystem functioning to wildfires using satellite-derived metrics of post-fire trajectories

Bruno Marcos [a,b,c,*], João Gonçalves [a,c,d], Domingo Alcaraz-Segura [e,f,g], Mário Cunha [h,i], João P. Honrado [a,b,c]

[a] CIBIO, Centro de Investigação em Biodiversidade e Recursos Genéticos, InBIO Laboratório Associado, Campus de Vairão, Universidade do Porto, 4485-661 Vairão, Portugal
[b] Departamento de Biologia, Faculdade de Ciências, Universidade do Porto, 4099-002 Porto, Portugal
[c] BIOPOLIS Program in Genomics, Biodiversity and Land Planning, CIBIO, Campus de Vairão, 4485-661 Vairão, Portugal
[d] proMetheus – Research Unit in Materials, Energy and Environment for Sustainability, Instituto Politécnico de Viana do Castelo (IPVC), Avenida do Atlântico, n.° 644, 4900-348 Viana do Castelo, Portugal
[e] iecolab. Interuniversity Institute for Earth System Research (IISTA), University of Granada, Av. del Mediterráneo, 18006 Granada, Spain
[f] Dept. of Botany, Faculty of Sciences, University of Granada, Av. Fuentenueva, 18071 Granada, Spain
[g] Andalusian Center for the Assessment and Monitoring of Global Change (CAESCG), Universidad de Almería, Crta. San Urbano, 04120 Almería, Spain
[h] Departamento de Geociências, Ambiente e Ordenamento do Território, Faculdade de Ciências, Universidade do Porto, 4099-002 Porto, Portugal
[i] Institute for Systems and Computer Engineering, Technology and Science (INESC TEC), Campus da Faculdade de Engenharia da Universidade do Porto, Rua Dr. Roberto Frias, Porto 4200-465, Portugal

ARTICLE INFO

Edited by Marie Weiss

Keywords:
Ecological disturbance
Ecological resilience
Post-fire recovery
Satellite image time-series
Tasseled cap transformation
Land surface temperature

ABSTRACT

Wildfire disturbances can profoundly impact many aspects of both ecosystem functioning and resilience. This study proposes a satellite-based approach to assess ecosystem resilience to wildfires based on post-fire trajectories of four key functional dimensions of ecosystems related to carbon, water, and energy exchanges: (i) vegetation primary production; (ii) vegetation and soil water content; (iii) land surface albedo; and (iv) land surface sensible heat. For each dimension, several metrics extracted from satellite image time-series, at the short, medium and long-term, describe both resistance (the ability to withstand environmental disturbances) and recovery (the ability to pull back towards equilibrium). We used MODIS data for 2000–2018 to analyze trajectories after the 2005 wildfires in NW Iberian Peninsula. Primary production exhibited low resistance, with abrupt breaks immediately after the fire, but rapid recoveries, starting within six months after the fire and reaching stable pre-fire levels two years after. Loss of water content after the fire showed slightly higher resistance but slower and more gradual recoveries than primary production. On the other hand, albedo exhibited varying levels of resistance and recovery, with post-fire breaks often followed by increases to levels above pre-fire within the first two years, but sometimes with effects that persisted for many years. Finally, wildfire effects on sensible heat were generally more transient, with effects starting to dissipate after one year and overall rapid recoveries. Our approach was able to successfully depict key features of post-fire processes of ecosystem functioning at different timeframes. The added value of our multi-indicator approach for analyzing ecosystem resilience to wildfires was highlighted by the independence and complementarity among the proposed indicators targeting four dimensions of ecosystem functioning. We argue that such approaches can provide an enhanced characterization of ecosystem resilience to disturbances, ultimately upholding promising implications for post-fire ecosystem management and targeting different dimensions of ecosystem functioning.

1. Introduction

Wildfire disturbances are projected to increase in both intensity and frequency in the future, exacerbated by shifts in global climate (Bowman et al., 2009; Kitzberger et al., 2017), as well as in land use and forest management (Tedim et al., 2013). Such disturbances can profoundly

* Corresponding author at: CIBIO, Centro de Investigação em Biodiversidade e Recursos Genéticos, InBIO Laboratório Associado, Campus de Vairão, Universidade do Porto, 4485-661 Vairão, Portugal.
E-mail address: bruno.marcos@cibio.up.pt (B. Marcos).

https://doi.org/10.1016/j.rse.2022.113441
Received 21 February 2022; Received in revised form 16 November 2022; Accepted 27 December 2022
Available online 2 January 2023

impact many aspects of the structure, composition, and functioning of ecosystems, despite being regarded as an integral part of their natural dynamics in several biomes (Adámek et al., 2016; San-Miguel-Ayanz et al., 2013). Furthermore, wildfires can decrease ecosystems' resistance to external disturbances and self-repairing capacity, eroding their resilience (Folke et al., 2004; Johnstone et al., 2010; Scheffer et al., 2015). Thorough assessments of the consequences of wildfire disturbances on ecosystems, as well as their responses and resilience to those disturbances, are thus needed to bridge gaps between science, policy, and management (Baho et al., 2017; Gouveia et al., 2010; van Leeuwen et al., 2010).

In this regard, several measures based on concepts related to ecosystem stability — such as "resilience", "resistance", and "recovery" — have been increasingly used to characterize both the effects of and the responses to wildfire disturbances in ecosystems. Traditionally, "resilience" was often quantified by measuring the speed at which an ecosystem returns to the original equilibrium, after disturbance (Meng et al., 2021). This measure concentrates on stability near that equilibrium, which is connected to the concept of "engineering resilience". This notion of resilience assumes that only one stable state exists, focusing on maintaining functioning efficiency (Holling, 1996, 1973).

However, as the use of the term "resilience" in the context of wildfires has increased in both research and management documents (Selles and Rissman, 2020), our understanding of resilience has been continuously advancing, which led to this notion being gradually replaced by the broader concept of "ecological resilience" (Elmqvist et al., 2003; Falk et al., 2022; Fan et al., 2021; Millar et al., 2007). This updated view of resilience explicitly recognizes the possibility of disturbances triggering sudden regime shifts when critical thresholds (or "tipping points") are exceeded (Scheffer et al., 2009, 2012), leading to alternative stable states (Boettiger et al., 2013; Scheffer and Carpenter, 2003). Ecosystems may thus endure critical transitions leading to their reconfiguration from one dynamic equilibrium state (i.e., the basin of attraction near which they tend to fluctuate; Scheffer et al., 2009) to an alternative contrasting stable state (e.g., Dwomoh and Wimberly, 2017; Hirota et al., 2011), mediated through adaptive capacity (Andersen et al., 2009). Ecological resilience can hence be regarded as the property mediating the transition among multiple stable states (Coop et al., 2020; Gunderson, 2000). Furthermore, ecological resilience focuses on maintaining functioning existence — rather than its efficiency (Holling, 1973, 1996). In a hierarchical perspective of resilience, engineering resilience can thus be associated with a higher level of persistence than ecological resilience (Delettre, 2021). Nonetheless, both "engineering resilience" and "ecological resilience" can be regarded as two different but complementary perspectives (Ingrisch and Bahn, 2018) — corresponding to two different types — of ecosystem resilience (Delettre, 2021).

In recent years, ecosystem resilience has been considered in two independent components — "resistance" and "recovery" (Coop et al., 2020; Falk, 2017; Falk et al., 2022; Fan et al., 2021; Millar et al., 2007). The concept of "resistance" expresses the ability of ecosystems to withstand environmental disturbances (De Keersmaecker et al., 2015) and is related to an instantaneous impact of exogenous disturbance on the ecosystem state (Hodgson et al., 2015). Resistance to wildfire disturbances can thus be measured by the magnitude of ecosystem changes following those disturbances (Meng et al., 2021), which can also correspond to a definition of burn severity (De Keersmaecker et al., 2015). On the other hand, "recovery" captures the endogenous processes that pull the disturbed system back towards equilibrium (Hodgson et al., 2015). Recovery can be measured by the duration of the period from a disturbed to a stable state (i.e., return time, as in the classical definition of resilience; Hodgson et al., 2015), even if this stable state does not fully correspond to pre-fire conditions. As regime shifts and critical transitions imply changes in ecosystem functions and services — with subsequent impacts on human societies (Folke et al., 2004). The ability to assess ecosystem state and resilience is thus critical for effective resource exploitation and ecosystem management (North et al., 2019; Meng et al., 2021).

Within the alterations induced by wildfires on the different components of ecosystems — i.e., structure, composition, and functioning —, functional attributes are of particular interest, because of their quick responses to disturbances than structural or compositional ones, and their more direct connections to ecosystem services (Alcaraz-Segura et al., 2008). Indeed, fire can cause rapid modifications in multiple dimensions of matter and energy flows in ecosystems (Falk et al., 2019; Marcos et al., 2021; Petropoulos et al., 2009). For instance, wildfires play an important role in the terrestrial biosphere carbon cycle (Wei et al., 2018), such as in biomass (Pellegrini et al., 2018; Sparks et al., 2018), and primary production (Leys et al., 2016). Furthermore, water supply and quality (Carvalho-Santos et al., 2019; Santos et al., 2015; Smith et al., 2011), as well as soil moisture and vegetation water content (Ebel and Martin, 2017; McGuire and Youberg, 2019; Senf and Seidl, 2020), can also be directly or indirectly affected by wildfire disturbances. Moreover, different aspects of energy balances, such as albedo (e.g., French et al., 2016; Gatebe et al., 2014; Quintano et al., 2019; Saha et al., 2017), latent heat (e.g., Sun et al., 2019), and sensible heat (e.g., Liu et al., 2018a; Maffei et al., 2018) can also suffer profound alterations induced by wildfires. Nonetheless, few studies have addressed wildfire effects on multiple dimensions of ecosystem functioning (however, see Marcos et al., 2021). Indeed, since both wildfire disturbances and resilience are multi-dimensional (Donohue et al., 2013, 2016), and post-fire trajectories of each dimension of ecosystem functioning are different (Ryu et al., 2018), more comprehensive indicators are still needed to understand post-fire processes better.

Due to lower costs and improved technology for providing up-to-date information on the status of ecosystem resources, remote sensing (RS) techniques have been increasingly employed to assess and monitor different aspects of the post-fire period (Lentile et al., 2006). Specifically, RS data has been used to map burned areas (Chuvieco et al., 2019; Giglio et al., 2018; Mouillot et al., 2014; Roy et al., 2019), as well as to assess and map both fire and burn severity (Marcos et al., 2021; Swetnam et al., 2021; Veraverbeke et al., 2011a). Post-fire recovery characterization has taken advantage of multi-temporal spectral data recorded from different space and airborne sensors, such as Landsat missions (Hope et al., 2007; van Leeuwen et al., 2010; Veraverbeke et al., 2012a; Viana-Soto et al., 2020), SPOT-Vegetation (Bastos et al., 2011; Gouveia et al., 2010), Terra/Aqua Moderate Resolution Imaging Spectroradiometer (MODIS) sensors (Caccamo et al., 2015; Hope et al., 2012; João et al., 2018), and multi-spectral cameras onboard Unoccupied Aircraft Systems (UAS; Samiappan et al., 2019). Furthermore, the utility of RS to evaluate resilience to wildfire disturbances has received increased attention, although mostly focusing on the "engineering resilience" paradigm (e.g., Bisson et al., 2008; Cui et al., 2013; Di Mauro et al., 2014; Díaz-Delgado et al., 2002; Dwomoh and Wimberly, 2017; Fernandez-Manso et al., 2016; Harris et al., 2014; Prodon and Diaz-Delgado, 2021; Spasojevic et al., 2016; Staal et al., 2018). On the other hand, indicators derived from satellite image time-series (SITS) can provide information on the dynamics of multiple dimensions of ecosystem functioning, thus enabling in-depth and integrative characterizations of ecosystem resilience to wildfires (João et al., 2018; Marcos et al., 2019). Notwithstanding, ecosystem functioning is largely not considered in most post-fire resilience assessments based on RS data (Frazier et al., 2013). The ability to assess and map the spatially and temporally heterogeneous effects of wildfire disturbances on ecosystem functioning and the responses and resilience of ecosystems to those disturbances makes RS data a major asset for risk assessment and governance, and also for post-fire restoration and management (Keeley, 2009; Parks et al., 2019; Smith et al., 2014; Tedim et al., 2013).

In this study, we propose a satellite-based approach for an enhanced assessment of ecosystem resilience following wildfire disturbances, on four key dimensions of ecosystem functioning related to the carbon, water, and energy exchanges: (i) vegetation primary production; (ii)

vegetation and soil water content; (iii) land surface albedo; and (iv) land surface sensible heat. To do so, we used several SITS extracted from MODIS data, as surrogates for those four dimensions of ecosystem functioning. We then illustrate how four metrics describing the short-, medium-, and long-term features of post-fire trajectories of those SITS can characterize different aspects related to both resistance (i.e., fire severity) and recovery for the four key and complementary dimensions of ecosystem functioning analyzed. Finally, we discuss the potential and added value of the proposed approach to improve satellite-based characterization of ecosystem resilience to wildfire disturbances over multiple dimensions of ecosystem functioning.

2. Methods

2.1. Study area

To illustrate our approach, we analyzed all areas burned in 2005, in the northwest Iberian Peninsula (NW-IP; Fig. 1). This area has one of the highest densities of ignitions among southern European countries, and one of the highest annual values of burned area in Europe (Catry et al., 2009), despite the enormous investments in fire suppression (Moreira et al., 2020). The year 2005 was particularly devastating in NW-IP, with over 340,000 ha burned (almost 4% of the study area), coinciding with severe drought (Bastos et al., 2011). This focal year was also chosen for the availability of SITS for more than a decade following the fire occurrences.

The NW-IP features diverse environmental characteristics, with strong environmental gradients, and a major biogeographic transition, from the Atlantic climate with temperate mixed and deciduous broadleaf forests in the north and west to the Mediterranean climate with evergreen sclerophyllous vegetation towards the southeast. Major land cover classes include shrublands in different successional stages, and plantation forests such as eucalypts, maritime pine, and mixed stands. Increasing fuel load and continuity, along with historical use of fire for agrosilvopastoral purposes, and extensive abandonment of farming and husbandry, have turned this area into a highly fire-prone landscape, and a hotspot in terms of wildfire occurrences, within the European context, in the last decades.

2.2. Satellite data preprocessing

To characterize ecosystem resilience to wildfire disturbances, we propose the use of indicators that inform on essential aspects of post-fire processes, extracted from the post-fire trajectories of satellite image time-series (SITS). To that end, SITS of the three Tasseled Cap Transformation (TCT) features of "Greenness" (TCTG), "Wetness" (TCTW), and "Brightness" (TCTB), as well as land surface temperature (LST), were used. These SITS were extracted from data products from the Moderate Resolution Imaging Spectroradiometer (MODIS) onboard the Terra satellite, for the years ranging from 2000 to 2018. Despite its relatively coarse spatial resolutions, both MODIS' archive length and its high temporal resolutions translate into a high potential to derive

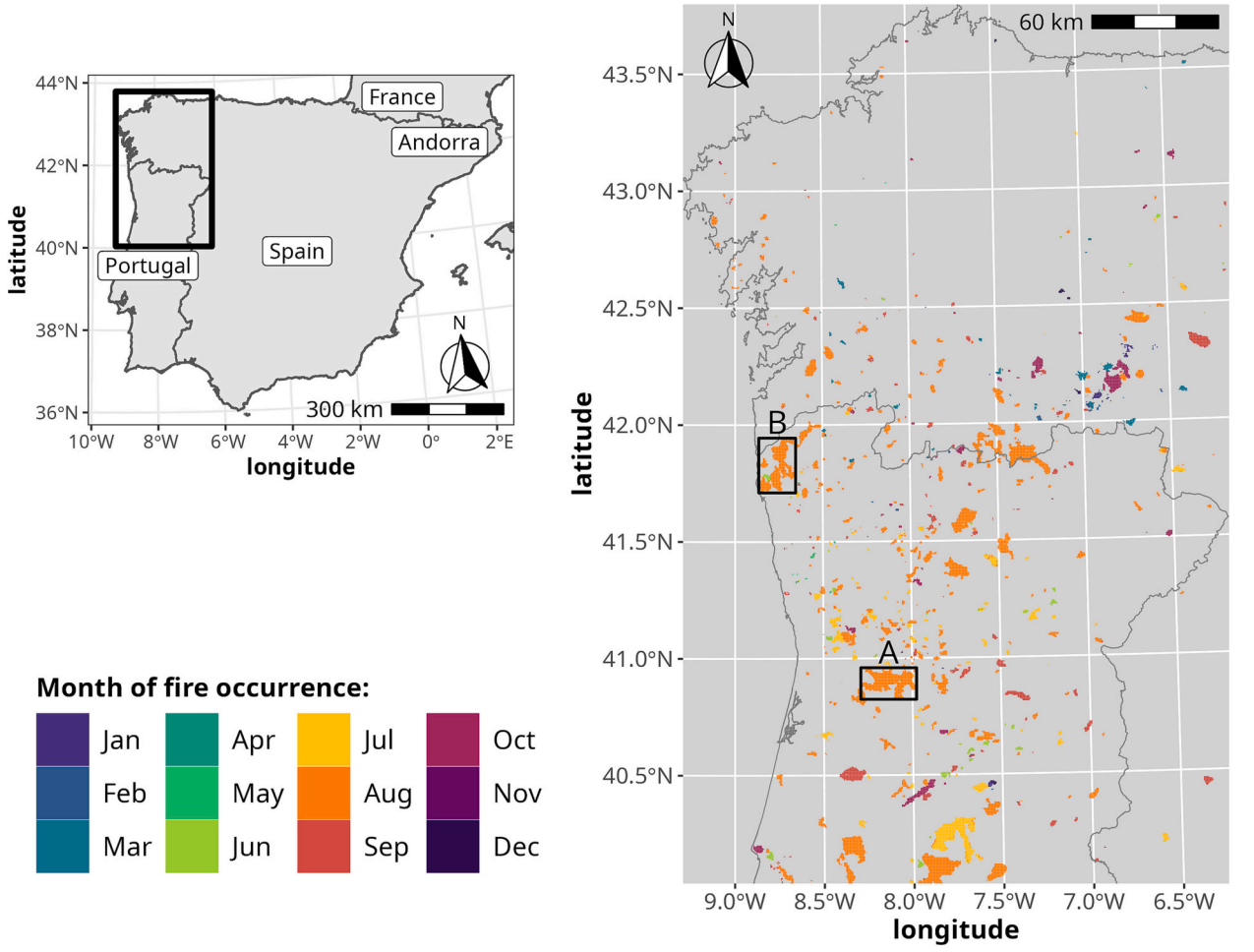

Fig. 1. The study area within the geographical context of the northwest Iberian Peninsula (top left); and the month of occurrence for burned patches resulting from wildfire events in the study area in 2005 (right, with the legend in the bottom left; extracted from the MODIS MCD64A1 "Burned Areas" product). Areas labeled "A" and "B" were used to illustrate the obtained results at local scales.

precise temporal estimations in the short, medium, and long terms.

The three TCT features are sensor-specific linear combinations of bands in the visible, near-infrared, and short-wave infrared regions of the electromagnetic spectrum (Lobser and Cohen, 2007). To compute these TCT features, principal component axes derived from a global sample are rotated to maximize the association of each axis with biophysical parameters such as the amount of photosynthetically active vegetation ("Greenness"), vegetation water content, and soil moisture ("Wetness"), and albedo ("Brightness"), respectively (Mildrexler et al., 2009). These variables, in turn, can be used as proxies for primary production, water content, and albedo, respectively (Marcos et al., 2021). We computed these TCT features for our study area by combining the seven bands available within the Terra Surface Reflectance product (MOD09A1; 8-Day L3 Global 500 m, Collection 6; Vermote, 2015), using the "rasterio" Python package (Gillies et al., 2013), with the coefficients used in previous work (Marcos et al., 2019, 2021; originally from Lobser and Cohen, 2007).

The LST is a calibrated measure of the thermal emissivity of the land surface (Duan et al., 2019), and therefore is a well-known proxy of sensible heat. The day LST from the Terra Land Surface Temperature/Emissivity product (MOD11A2; 8-Day L3 Global 1000 m, Collection 6; Wan et al., 2015) was rescaled to degrees Celsius, using the "rasterio" Python package (Gillies et al., 2013). Finally, to correct spurious values in SITS of LST and the three TCT features, a pixel-wise filtering procedure based on the Hampel identifier (Hampel, 1971, 1974) was implemented and applied within the R statistical programming environment (R Core Team, 2021).

Together, the four RS-based surrogates used — TCTG, TCTW, TCTB, and LST — can inform on the four key aspects of matter and energy flows in ecosystems (i.e., ecosystem functioning): primary production, water content, surface albedo, and sensible heat, respectively, and have been successfully used in prior studies involving fire-related applications (e.g., Bowman et al., 2015; Coops et al., 2008; Marcos et al., 2019, 2021; Quintano et al., 2015; San-Miguel-Ayanz et al., 2013).

To identify areas that burned in 2005, within the study area, with a contiguous area above 100 ha (i.e., "big fires"), we used the Terra+Aqua Burned Area product (MCD64A1; monthly L3 Global 500 m, Collection 6; Giglio et al., 2018), following the procedures described in previous works (see Marcos et al., 2019).

Data processing and analysis tasks were generally undertaken within the R statistical programming environment, using mainly the "raster" package (Hijmans, 2020). All three MODIS products covering the study area (i.e., MODIS tile h17v04) were initially downloaded and reprojected to the WGS84/UTM29N coordinate system using the "MODIStsp" R package (Busetto and Ranghetti, 2016).

2.3. Time-series decomposition and normalization

Meaningful post-fire resilience metrics can be extracted from SITS, provided that seasonal variations (i.e., fluctuations in the data with a fixed and known frequency) are first separated from long-term changes due to wildfire disturbances. To that end, we used the "Seasonal and Trend decomposition using Loess" (STL) algorithm for time-series additive decomposition. STL is a robust and versatile method that uses the loess smoother to extract the seasonal, trend, and remainder components of a time-series (Cleveland et al., 1990), as described by the following expression:

$$y_t = S_t + T_t + R_t \quad (1)$$

where y_t is the original time series S_t is the seasonal component, T_t is the trend component, and R_t is the remainder component, all at period t and with the same units.

In our approach, we applied STL decomposition to obtain seasonally adjusted time-series — corresponding to the original time-series with the seasonal component removed —, to establish pre-fire reference conditions, since it is considered useful for estimating both non-seasonal variability and central tendencies, and can include noise and other non-seasonal, non-cyclic fluctuations — such as abrupt shifts related to distinct disturbances (Hyndman and Athanasopoulos, 2018). Additionally, we used the trend component to calculate moving-window medians, which represent incremental steps in the post-fire trajectories and aim to support the extraction of metrics of post-fire resilience. This time-series component includes both the long-term variation in the data and cyclic effects (i.e., fluctuations in the data that are not of a fixed frequency), and is equivalent to removing the remainder component from the seasonally adjusted time series.

Among the STL decomposition procedure parameters, "t.window" and "s.window" play a crucial role, since these two parameters control how rapidly the trend and seasonal components can change. The "t.window" and "s.window" parameters correspond to the span (in lags) of the "loess" window for trend and seasonal extraction, respectively, and should both be odd numbers, as described in Cleveland et al. (1990). In our illustrative test case, we used a value of 47 (i.e., the nearest odd number above the number of observations in each year, in MODIS products with 8-day temporal resolution) for both the "t.window" and "s.window" parameters. This value seemed to correspond to a compromise that allowed to capture a wide range of effects in the short (i.e., less than one year), medium (i.e., up to three years), and long terms (i.e., above three years), for post-fire analysis. The width of the moving windows was also fixed to the same value as "t.window" and "s.window" (i.e., 47) since it corresponds to approximately one year of observations. Additionally, we opted for using robust fitting (i.e., "robust" parameter = TRUE) to reduce the effect of occasional unusual observations on the trend and seasonal components. All the remaining parameters of the STL procedure were fixed at their respective default values.

Finally, we defined the pre-fire reference intervals (see Fig. 2) to be within one median absolute deviation from the median (i.e., median ± 1 M.A.D.), using all values of the seasonally-adjusted time-series within three years before the date of the fire occurrence, to reduce the impact of extreme values.

2.4. Extraction of metrics from post-fire trajectories

To support the assessment and characterization of key features of both resistance and recovery of ecosystem functioning to wildfire disturbances, we derived several metrics from satellite-based post-fire trajectories from the decomposed time series.

Firstly, for the extraction of metrics of post-fire short-term effects, the date of the first directionality inflection in the trend component curve, t_{INF}, after the date of the wildfire occurrence (t_{FIRE}) was determined, for each pixel and across each of the four dimensions of ecosystem functioning. By representing the first major change of directionality — from divergent to convergent with the pre-fire conditions —, this moment in the post-fire period can be regarded as an approximation to the date of the start of recovery. The duration of the period between t_{FIRE} and t_{INF} — called "Directionality Inflection Time" (DIT) — can thus be linked to short-term recovery speed. Additionally, this metric is also related to ecosystem resistance to wildfire disturbances, since it estimates the duration of the period in which a particular dimension of ecosystem functioning is under disturbance.

The "S95" metric is defined as the difference between the pre-fire median and the 95% percentile of the seasonally adjusted time-series values within the first moving window immediately after a fire. As an estimate of the near-maximum short-term impact of the wildfire disturbance on the corresponding dimension of ecosystem functioning, this metric can be used as a measure of wildfire disturbance severity, as well as to indicate the level of ecosystem resistance to those disturbances (De Keersmaecker et al., 2015; Meng et al., 2021).

Next, to portray the medium-to-long term responses of ecosystem functioning to wildfire disturbances, we propose two related but independent "return time"-type metrics extracted from post-fire trajectories.

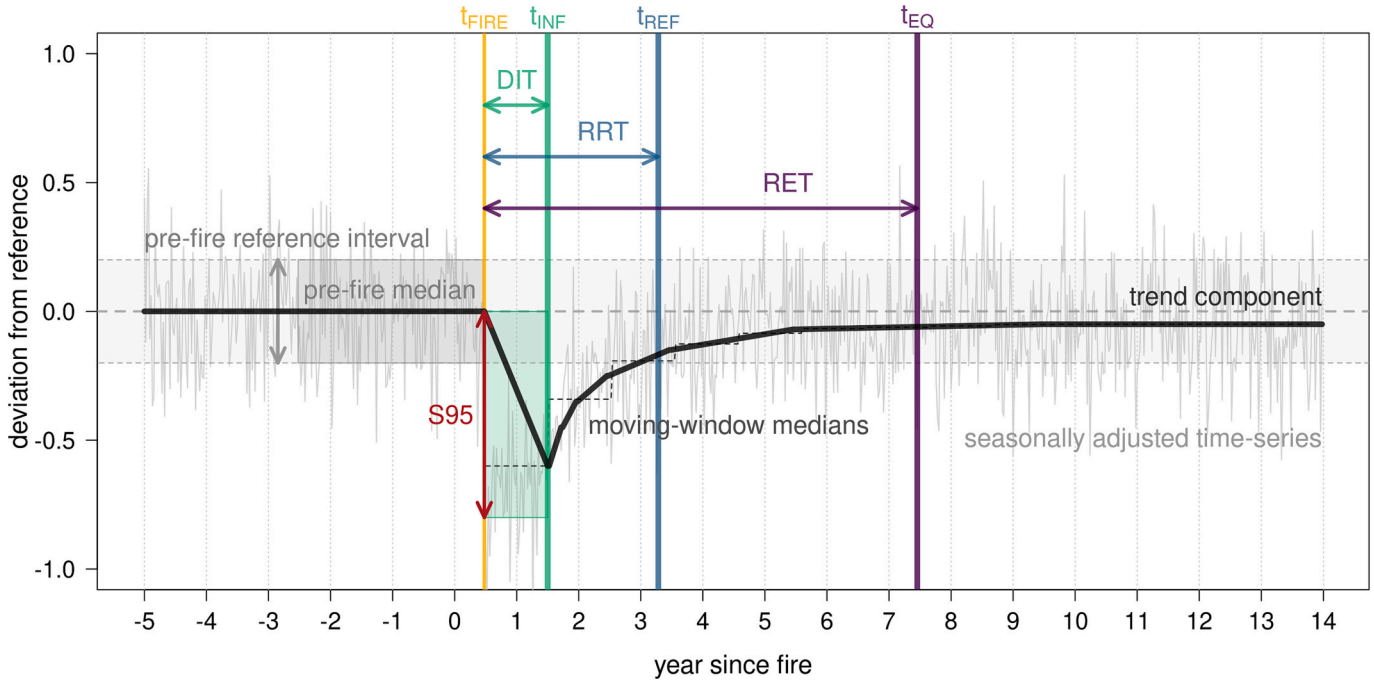

Fig. 2. Illustration of the satellite-derived metrics of ecosystem resilience used in this study, extracted from a generic representation of a post-fire trajectory. The "S95" metric measures the difference between the 95% quantile immediately after the fire and the pre-fire reference value, providing an estimate of wildfire severity related to ecosystem resistance. The "DIT", "RRT", and "RET" metrics measure the amount of time between the date of the fire occurrence (t_{FIRE}) and the dates of post-fire directionality inflection (t_{INF}), return-to-reference (t_{REF}), and return-to-equilibrium (t_{EQ}), respectively. These metrics provide estimates of post-fire recovery speed in the short term (i.e., the start of recovery), and in the medium-to-long term (for both "engineering resilience" and "ecological resilience").

To this end, the "Return-to-Reference" and "Return-to-Equilibrium" dates (t_{REF} and t_{EQ}, respectively) have to be determined. The t_{REF} date — if successfully found — corresponds to the first moment, after t_{INF}, for which both the value of the trend component, as well as its corresponding moving window median, are both within the pre-fire reference interval. Both criteria must be met to minimize false detections caused by short-term oscillations. The duration of the period between t_{FIRE} and t_{REF} — called "Return-to-Reference Time" (RRT) — provides an estimate of the amount of time needed to achieve the pre-fire conditions once again (when applicable). This can be regarded as a medium-to-long term recovery speed metric that aligns with the concept of "engineering resilience" (Holling, 1996).

Finally, the t_{EQ} date — if successfully found — corresponds to the first of at least two consecutive moving window medians (after t_{INF}) that exhibit relative change rates below a predefined threshold — in the case of our illustrative test case, we used 5% as a fixed threshold in all cases, but other values could be used instead. From this date, the "Return-to-Equilibrium Time" (RET) metric — calculated as the duration of the period between t_{FIRE} and t_{EQ} — approximates the amount of time needed to achieve a stable state after a fire, which is a measure of long-term recovery speed. As this stable state can differ (although not necessarily) from pre-fire conditions, the RET metric can be regarded as being more in line with the concept of "ecological resilience" (Holling, 1996).

The full procedure to extract the aforementioned metrics from post-fire trajectories is illustrated in Fig. 2.

Using the 16 indicators resulting from applying those four metrics — S95, DIT, RRT, and RET —, to the four key and complementary dimensions of ecosystem functioning analyzed, we characterized all post-fire trajectories until 2018, for wildfires occurring in 2005 in the study area, in terms of ecosystem resistance and recovery to those disturbances. We then inter-compared the distributions of the 16 indicators (i.e., four metrics for each of four dimensions), and calculated pairwise Spearman rank correlations, to assess potential collinearity among indicators, using all complete pairwise observations.

3. Results

3.1. General patterns

The distributions of the four MODIS-derived metrics used to characterize the post-fire trajectories in our study area (i.e., S95, DIT, RRT, and RET), for each of the four aspects of ecosystem functioning considered — i.e., vegetation primary production (TCTG), vegetation and soil water content (TCTW), land surface albedo (TCTB), and land surface sensible heat (LST), are shown in Fig. 3.

The distributions obtained for the S95 metric of wildfire severity (Fig. 3a) showed the overall directionality of the short-term effects of wildfires, for each of the satellite-derived proxies of the four dimensions of ecosystem functioning. Namely, TCTG and TCTW decreased immediately after a fire, while LST increased. On the other hand, TCTB exhibited a well-marked multi-modal distribution, with one group corresponding to decreased values, whereas the other corresponded to increased values.

The distributions of the DIT metric of short-term recovery (Fig. 3b) obtained for TCTG, TCTW, and LST were mainly concentrated within the two first years after a fire, with lower values for TCTG, followed by TCTW and LST. As the DIT metric for TCTB, values were much more dispersed than the other dimensions, with low and high values within the first year and after two years following the fire.

The RRT metric of medium-to-long term recovery (Fig. 3c) had more tightly concentrated (i.e., less dispersed) distributions for TCTG and LST but more dispersed for TCTB and TCTW. Furthermore, while TCTB had more values concentrated in the first year after the fire than the other dimensions, TCTW was the dimension with the overall highest values for this metric (e.g., higher than four years after the fire).

Finally, distributions of the RET metric of long-term recovery (Fig. 3d) were more dispersed than for RRT. Overall, RET was higher for TCTG, followed by TCTW, and then TCTB. On the other hand, RET values of LST were generally the lowest.

As an example of the abovementioned regional-scale general

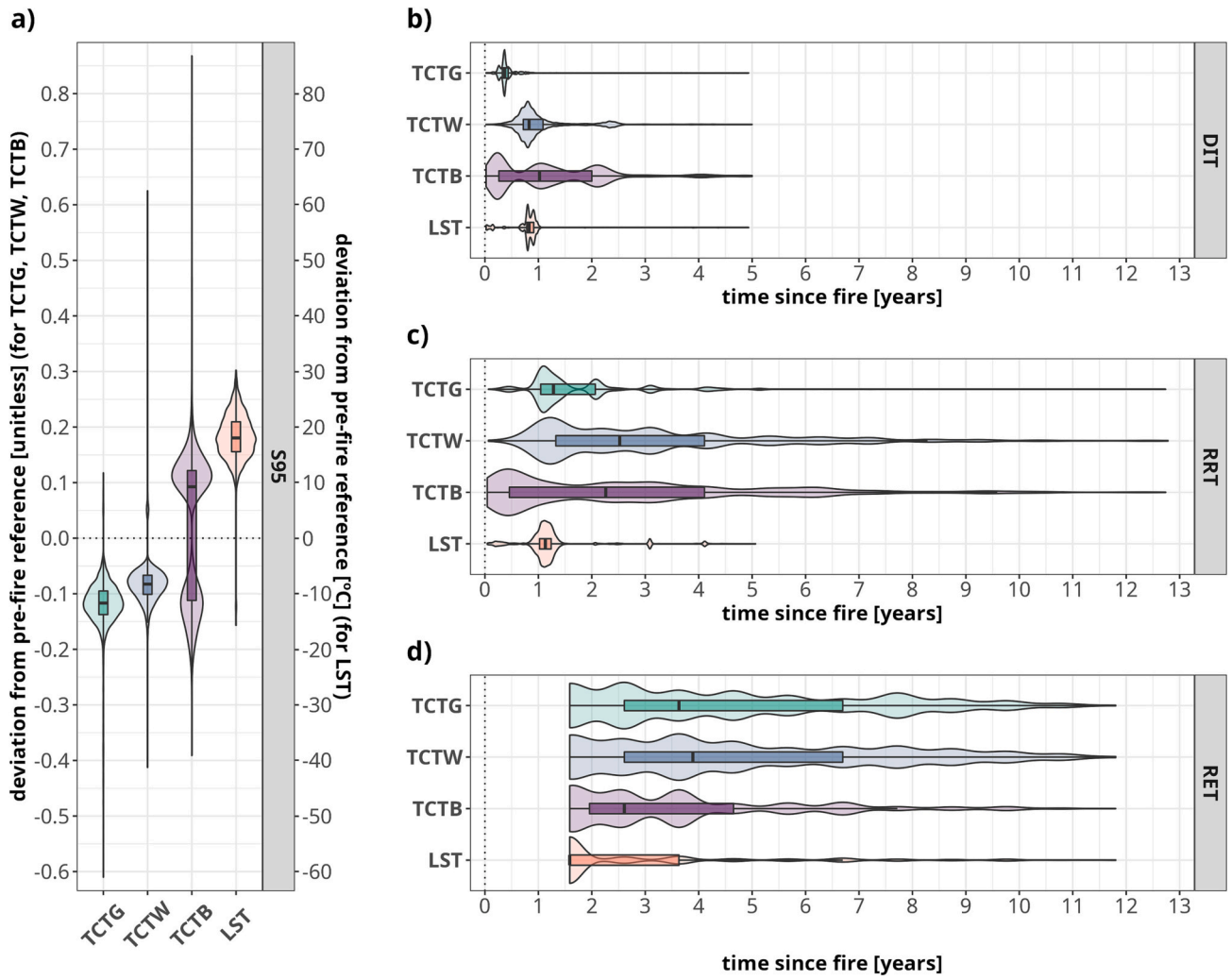

Fig. 3. Distributions (represented in combined box-violin plots) of the four MODIS-derived metrics, for all areas burned in 2005 (identified by the MODIS burned area product), in NW Iberian Peninsula, for each of the proxies of the four dimensions of ecosystem functioning: TCTG — Tasseled Cap Greenness for vegetation primary production, TCTW — Tasseled Cap Wetness for vegetation and soil water content, TCTB — Tasseled Cap Brightness for land surface albedo, and LST — Land Surface Temperature for land surface sensible heat. The metrics are the following: (a) the "95%-severity" ("S95") wildfire severity/resistance metric; (b) the "Directionality Inflection Time" ("DIT") metric of short-term recovery speed; (c) the "Return-to-Reference Time" ("RRT") metric of medium-to-long term recovery; and (d) the "Return-to-Equilibrium" ("RET") metric of long-term recovery.

patterns, both the spatial patterns (Fig. 4) and the overall multidimensional diagnostics (Fig. 5) obtained for the sixteen indicators used are shown for two local-scale specific burned areas.

3.2. Indicator inter-comparison

To show the independence among indicators, the Spearman rank correlations (ρ) between each pair of 16 indicators are presented in Table 1. The correlations obtained were overall low to moderate (i.e., $|\rho| \leq 0.50$), except for six pairs of indicators. Three of those moderate to high correlations were obtained for the pair RRT vs. RET, for LST ($\rho = 0.84$), TCTB ($\rho = 0.72$), and TCTW ($\rho = 0.57$), with 100% of the pairwise observations with valid values (i.e., $n = 13{,}751$; see Table S1 in Supplementary Material). The remaining three correlation values above $|\rho| = 0.50$ were obtained for the pairs S95 vs. DIT ($\rho = -0.65$), S95 vs. RRT ($\rho = 0.68$), and DIT vs. RRT ($\rho = 0.79$), all for TCTB. In the case of these last three pairs, the respective correlation values were calculated using only 62% of the total observations (i.e., $n = 8529$; see Table S1 in Supplementary Material). For the remainder observations ($n = 5222$), either t_{REF} or t_{EQ} (or both) were not detected, corresponding to pixels in which at least one of the following situations apply: (i) the values of the trend component did not cross the pre-fire reference interval until the end of the analyzed period – corresponding to a range between 2% of the pixels (LST) and 24% of the pixels (TCTB); and (ii) a relative change between consecutive moving windows below the predefined threshold was never achieved until the end of the analyzed period (for up to 2% of the cases for TCTB). Finally, it should also be noted that all the six values considered moderately to highly correlated were found for pairs in which both indicators belonged to the same ecosystem functioning dimension.

4. Discussion

4.1. Multidimensional patterns of post-fire resilience in NW Iberian Peninsula

4.1.1. Vegetation primary production

Overall, post-fire trajectories of TCTG in NW-IP exhibited the typical pattern observed in temporal profiles of remotely-sensed vegetation indices (e.g., García-Llamas et al., 2019; Veraverbeke et al., 2011b). Abrupt breaks (translated by the obtained values for the S95 metric) resulting from the sudden removal of green vegetation caused by

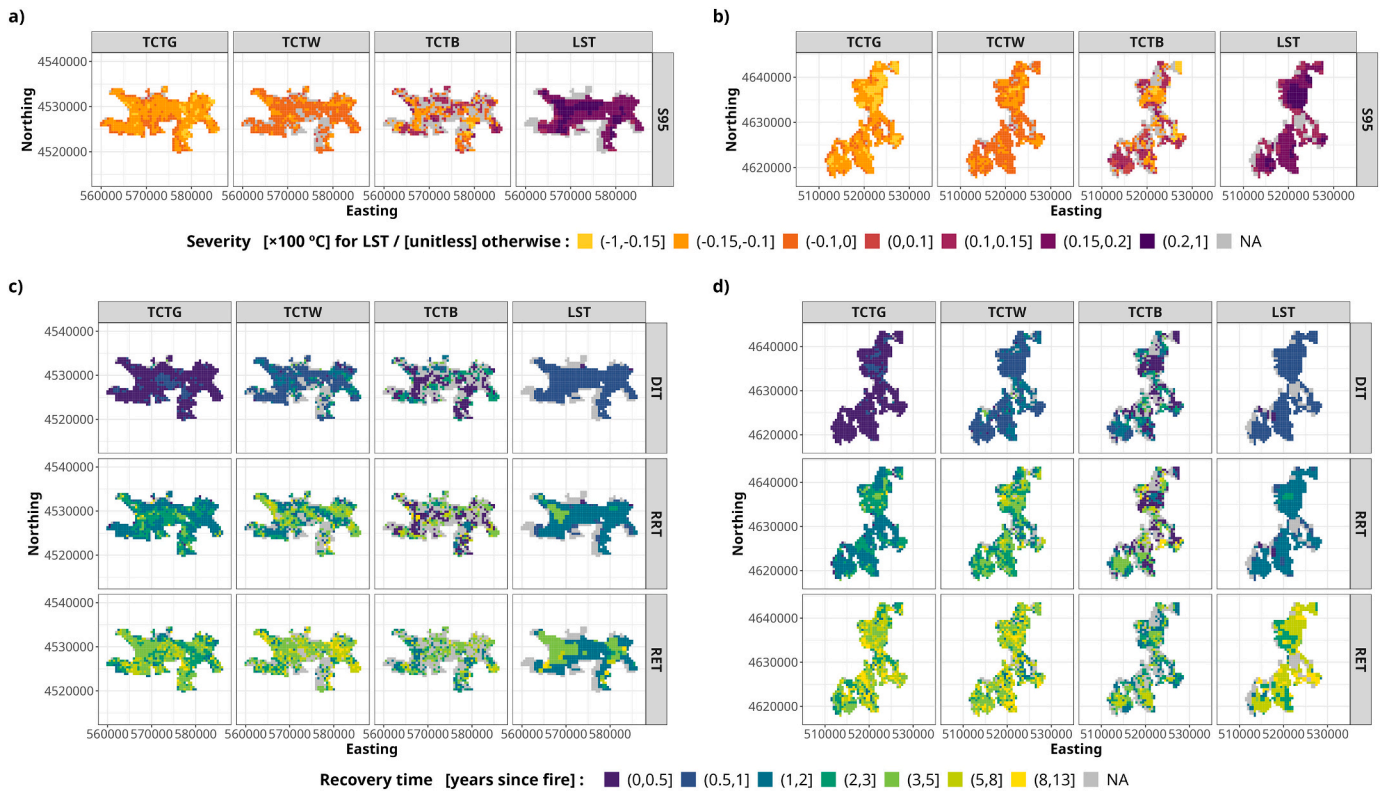

Fig. 4. Example of spatialized post-fire trajectory-based metrics of resilience proposed in this study, for two different burned areas — one on the left (a, c), and the other on the right (b, d). For each of the satellite-derived proxies of the four dimensions of ecosystem functioning: TCTG — Tasseled Cap Greenness for vegetation primary production, TCTW — Tasseled Cap Wetness for vegetation and soil water content, TCTB — Tasseled Cap Brightness for land surface albedo, and LST — Land Surface Temperature for land surface sensible heat, the following metrics are presented: (a, b) the "95%-severity" ("S95") wildfire severity/resistance metric; and (c, d) the three metrics of post-fire recovery at short, medium, and long terms, respectively – "Directionality Inflection Time" ("DIT"; top row), "Return-to-Reference Time" ("RRT"; middle row), and "Return-to-Equilibrium" ("RET"; bottom row). Note that all legend intervals are both left open and right closed, as denoted by "(" and "]", respectively.

wildfire disturbances were followed by relatively steep recoveries, usually starting in the first six months after the fire (as suggested by the distribution of the DIT metric — see Fig. 3b).

The sudden vegetation removal that follows wildfires corresponds, in the short term, to a cessation of ecosystem carbon uptake induced by the shutdown, death, and shedding — besides the actual combustion — of leaves within the canopy (Beringer et al., 2003), leading to substantial losses in primary production and biomass (Leys et al., 2016; Pellegrini et al., 2018; Sparks et al., 2018). Furthermore, early post-fire responses are — as found in previous works (e.g., João et al., 2018) —, highly dependent on suitable abiotic conditions such as post-fire climate (e.g., precipitation, temperature), as well as biotic factors. These biotic factors are usually related to vegetation composition, such as the relative abundance of seeders and resprouters (Arnan et al., 2007; Day et al., 2020; Parra and Moreno, 2018; Prior and Bowman, 2020; Tiribelli et al., 2018), and is mediated by fire characteristics of the fire regime, such as severity and frequency (Díaz-Delgado et al., 2002), and their spatial heterogeneity (Kolden et al., 2012; Meddens et al., 2018).

In the medium-to-long term, the distributions obtained for the RRT and RET metrics for TCTG suggest that pre-fire reference levels were usually reached within the first two years following the fire. After this period, the response speed gradually decreased into eventual stabilization in the subsequent years, which is in line with previous studies for this region (Bastos et al., 2011; Gouveia et al., 2010; João et al., 2018). Moreover, these patterns may be influenced mainly by fire severity and vegetation composition (Day et al., 2020; Díaz-Delgado et al., 2002; Meng et al., 2018; Tiribelli et al., 2018; van Leeuwen et al., 2010). In some cases, studies have shown that fire can even induce the regeneration of several species and contribute to replacing older, drier, and unhealthier individuals with more productive saplings (Oliveira et al., 2012; Semeraro et al., 2019). However, the effect of species traits and interannual variations in climate tend to be averaged out, eventually reducing the differences between vegetation types in the long term (Johnstone et al., 2010).

4.1.2. *Vegetation and soil water content*

Compared to TCTG, TCTW exhibited temporally more delayed effects in post-fire trajectories in NW-IP (translated by the DIT metric), as were previously reported (e.g., Marcos et al., 2021). These patterns can be associated with the following major effects, which can persist for up to one year after the fire: (i) changes in vegetation structure (Hansen et al., 2001; Nguyen et al., 2018); (ii) increased quantities of impervious materials such as ashes, char, and soot (Bodí et al., 2014; Ramanathan and Carmichael, 2008), which lead to decreased water retention capacity and increased soil water repellency, post-fire runoff, and erosion rates (Hubbert et al., 2012; MacDonald and Huffman, 2004); and (iii) loss of foliar moisture leading to increased vegetation mortality (Lobser and Cohen, 2007; Senf and Seidl, 2020; Viana-Soto et al., 2020), due to fire-related damage leading to leaf shut down (Beringer et al., 2003; Senf and Seidl, 2020).

In the medium-to-long term, TCTW generally recovered following: (i) the increase in canopy structural complexity associated with vegetation regeneration (Nguyen et al., 2018); and (ii) the decrease in concentrations of impervious soil materials. The distributions of RRT and RET for NW-IP suggest that post-fire recovery of water content was slower and more gradual than that of primary production. While this is in line with some studies (e.g., Viana-Soto et al., 2020), the opposite relationship has also been observed, although using different spectral

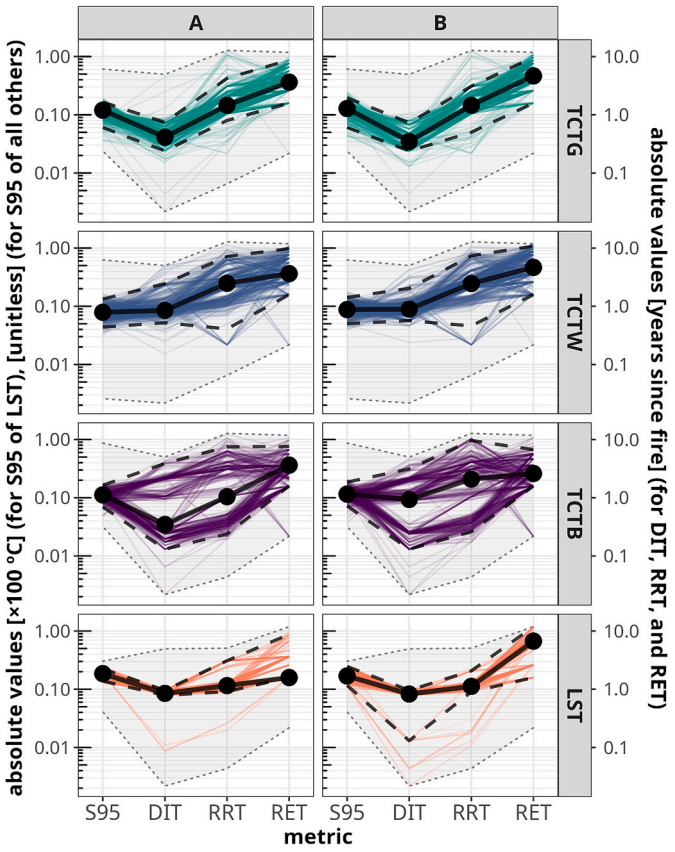

Fig. 5. Example of a representation of the overall multidimensional diagnostics based on the metrics of resilience proposed in this study for two different burned areas (A and B in Fig. 1). For each of the satellite-derived satellite-derived proxies of the four dimensions of ecosystem functioning: TCTG — Tasseled Cap Greenness for vegetation primary production, TCTW — Tasseled Cap Wetness for vegetation and soil water content, TCTB — Tasseled Cap Brightness for land surface albedo, and LST — Land Surface Temperature for land surface sensible heat, the following metrics are presented: (i) the "95%-severity" ("S95") wildfire severity/resistance metric; and the three metrics of post-fire recovery at short, medium, and long terms, respectively – (ii) "Directionality Inflection Time" ("DIT"); (iii) "Return-to-Reference Time" ("RRT"); and (iv) "Return-to-Equilibrium" ("RET"). In each panel, big dots connected by solid black lines represent the median values of each metric for that particular burned area; dashed black lines connect the 2.5% and 97.5% percentiles of the distribution of each metric across all pixels for that particular burned area, and dotted gray lines delimiting shaded areas connect the overall minimum and maximum values of the distribution of each metric for all areas burned in 2005 in the northwestern Iberian Peninsula. In these plots, higher values correspond to lower resistance (S95) or recovery rates at short (DIT), medium-to-long (RRT), and long (RET) terms.

indices (e.g., Ryu et al., 2018). Furthermore, differences in post-fire water content may be associated with decreased moisture retention ability of vegetation and soils, increased fuel flammability and fire risk (Pausas and Paula, 2012), and lower resilience capacity, especially when associated with post-fire drought conditions (Liu et al., 2021).

4.1.3. Land surface albedo

Overall, post-fire trajectories of TCTB exhibited dual directionality of the effects of the 2005 wildfire disturbances in NW-IP (as captured by the distributions of the S95 and DIT metrics) in albedo, which is coherent with previously reported findings (e.g., Marcos et al., 2021; Quintano et al., 2019; Ramanathan and Carmichael, 2008). These patterns can be explained mainly through post-fire changes in the relative abundance of land surfaces with distinct reflective properties (Lentile et al., 2006). More specifically, TCTB tends to decrease immediately after a fire, leading to a "darkening" effect due to an increased concentration of black carbon in soot and char, which absorbs visible solar radiation (Ramanathan and Carmichael, 2008). This effect tends to dissipate before significant vegetation regeneration, leading to a temporary "brightening" effect one to two years after fire (Quintano et al., 2019; Saha et al., 2019).

Our results suggest that the inflection point (t_{INF}) corresponding to only one of the two effects — either "darkening" or "brightening", but not both —, was detected. This implies that the RRT metric for TCTB captured the rate at which either: (i) pre-fire reference levels were reached (or crossed), corresponding to decreasing concentrations of char and soot, before eventually approaching "brightening"; or (ii) the transition from the "brightening" effect to pre-fire reference levels was completed, suggesting the corresponding regeneration of vegetation. On the other hand, both "darkening" and "brightening" effects can sometimes persist for many years after the fire — as shown by the distribution of the RET metric for TCTB —, which can translate into a potential depletion of the ecosystem resilience capacity, previously observed in other studies (e.g., Gatebe et al., 2014; Saha et al., 2017).

4.1.4. Land surface sensible heat

Compared to the previous three dimensions of ecosystem functioning analyzed, wildfire disturbances seemed to have more transient effects on sensible heat (as captured by all four metrics used), which was previously reported in other studies (Marcos et al., 2018; Quintano et al., 2015; Zheng et al., 2016).

Increases in LST immediately following the fire (captured by the S95 metric) are usually direct consequences of vegetation removal, which leads to increases in the ratio of sensible-to-latent heat (Vlassova et al., 2014) due to a reduction in evapotranspiration (Beringer et al., 2003; Liu et al., 2018b). This effect tends to start dissipating around one year after fire (Liu et al., 2019), as was shown by the distribution of the DIT metric extracted from LST for NW-IP. Furthermore, LST tends to recover to pre-fire levels after one to two years following the fire (Veraverbeke et al., 2012b), which was translated by the distributions of the RRT and RET metrics.

Overall, our results suggest that sensible heat was highly resilient to the 2005 wildfire disturbances in NW-IP, since values of LST mostly either had their post-fire inflection points detected within the pre-fire reference interval — i.e., severity was low —, or they rapidly returned to pre-fire levels.

4.2. General considerations and future pathways

4.2.1. Multi-indicator approach

Our approach comprises four dimensions of ecosystem functioning and two components of resilience. Althogether, the four satellite-based metrics extracted from post-fire trajectories proposed in this study — i.e., S95, DIT, RRT, and RET — aimed to capture key aspects of post-fire trajectories in the short, medium, and long terms for each of the four dimensions of ecosystem functioning of primary production, vegetation water content and surface soil moisture, albedo, and sensible heat. Correlations between the resulting sixteen indicators (i.e., four metrics extracted for each of the four dimensions) were mainly low to moderate, suggesting a high degree of complementarity — rather than redundancy — among all indicators, even if a small degree of correlation between few different indicators was to be expected.

Other approaches have previously combined information extracted from satellite imagery corresponding to multiple dimensions of ecosystem functioning. For instance, the MODIS Global Disturbance Index (MGDI; Mildrexler et al., 2009) takes advantage of the contrasting post-disturbance trajectories of LST and the Enhanced Vegetation Index (EVI) to detect disturbances such as wildfires. On the other hand, combinations of Tasseled Cap "Brightness", "Greenness", and "Wetness" into synthetic disturbance indices (DI) have previously been used to map disturbances including wildfires (e.g., Healey et al., 2005). However, in

Table 1
Pairwise correlations between the indicators analyzed in this study, for complete pairwise observations (maximum n = 13,751), obtained for the four metrics proposed in this study, and for each of the satellite-derived proxies of the four dimensions of ecosystem functioning: TCTG — Tasseled Cap Greenness for vegetation primary production, TCTW — Tasseled Cap Wetness for vegetation and soil water content, TCTB — Tasseled Cap Brightness for land surface albedo, and LST — Land Surface Temperature for land surface sensible heat. The metrics are the following: S95 — "95%-severity" wildfire severity/resistance metric, DIT — "Directionality Inflection Time" metric of short-term recovery, RRT — "Return-to-Reference Time" metric of medium-term recovery, and RET — "Return-to-Equilibrium" metric of long-term recovery. Numbers in bold lettering and gray background highlight values of Spearman rank correlation of $|\rho| > 0.50$.

		TCTG				TCTW				TCTB				LST			
		S95	*DIT*	*RRT*	*RET*	*S95*	*DIT*	*RRT*	*RET*	*S95*	*DIT*	*RRT*	*RET*	*S95*	*DIT*	*RRT*	*RET*
LST	*RET*	0.26	0.15	0.34	0.15	0.28	−0.02	0.26	0.26	−0.00	−0.08	0.17	0.18	0.00	0.05	**0.84**	1.00
	RRT	0.27	0.18	0.46	0.18	0.31	0.06	0.35	0.30	−0.01	−0.06	0.20	0.18	−0.44	0.46	1.00	
	DIT	−0.01	0.18	0.24	0.15	−0.02	0.31	0.11	0.04	0.15	−0.07	−0.08	−0.08	0.04	1.00		
	S95	−0.32	−0.13	−0.29	−0.05	−0.15	0.03	−0.06	−0.09	−0.07	0.10	−0.09	−0.17	1.00			
TCTB	*RET*	0.25	0.03	0.25	0.09	0.25	−0.06	0.28	0.28	−0.16	0.07	**0.72**	1.00				
	RRT	0.16	0.03	0.26	0.10	0.33	−0.08	0.39	0.28	**−0.68**	**0.79**	1.00					
	DIT	−0.25	−0.05	−0.08	−0.01	0.09	−0.05	0.11	0.01	**−0.65**	1.00						
	S95	0.28	0.10	0.11	0.02	−0.28	0.15	−0.19	−0.12	1.00							
TCTW	*RET*	0.26	0.12	0.0.33	0.11	0.21	0.06	**0.57**	1.00								
	RRT	0.20	0.11	0.41	0.16	0.29	0.36	1.00									
	DIT	−0.13	0.06	0.15	0.13	−0.10	1.00										
	S95	0.34	0.12	0.32	0.13	1.00											
TCTG	*RET*	0.04	0.05	0.33	1.00												
	RRT	0.29	0.40	1.00													
	DIT	0.15	1.00														
	S95	1.00															

contrast with disturbance indices such as the MGDI and the Tasseled Cap-based DI, our approach is characterized by: (i) allowing and facilitating analyses of the inherently multidimensional post-fire processes, without the inevitable information losses resulting from combining multiple satellite-based proxies into a single synthetic index; and (ii) better translating satellite-observations into ecologically more meaningful indicators of post-fire effects and responses, based on ecosystem functioning, towards increased operational and interpretable outputs.

For these reasons, we argue that the metrics proposed in this study are able to provide a relatively compact but comprehensive set of indicators to describe the complex patterns associated with post-fire effects on ecosystem functioning, as well as with ecosystems' responses to such disturbances. Nevertheless, a subset of the indicators proposed in this study can potentially be used in situations in which only a partial picture of the post-fire period is under focus, or when data availability or desired quality is limited — e.g., if only the short-term effects (i.e., severity) of wildfires on primary production are of interest.

4.2.2. Alternative data sources

Other sources of SITS — in addition to MODIS (e.g., Sentinel, Landsat) — can be used when applying the approach proposed in the present study. However, it should be noted that, depending on the specific goals, the length of the available image archives and the temporal resolution of the observations can be limiting factors — e.g., for establishing pre-fire reference periods, or to evaluate post-fire trajectories in longer timeframes. Indeed, because of known trade-offs between satellite-imagery characteristics such as spatial resolution (i.e., pixel size) and temporal frequency (i.e., the time between consecutive images), we argue that MODIS imagery currently still fits the purposes of our proposed approach well. Despite its moderate-to-coarse spatial resolutions (i.e., 250-1000 m), The high temporal resolutions of MODIS imagery (i.e., up to two daily observations) and a relatively long archive (starting in 2000) allow for enhanced temporal estimations of key features of post-fire trajectories, in the short, medium, and long terms. Although MODIS products will be affected by the drift of the Terra and Aqua satellites starting in 2022, other missions such as VIIRS and Sentinel-3 with comparable spectral, spatial, and temporal resolutions can provide continuity to the time-series used our study.

Moreover, alternative remotely sensed proxies could be used to characterize the four different dimensions of ecosystem functioning — such as the Normalized Difference Vegetation Index (NDVI), the Normalized Difference Water Index (NDWI), the Normalized Burned Ratio (NBR), or even pre-calibrated satellite-based products of albedo or soil moisture. However, we argue that SITS of LST and the TCT features of "Brightness", "Greenness", and "Wetness" — used in our illustrative test case — provide information on those four dimensions of ecosystem functioning in an efficient and transferable way, since they can be computed from a wide range of satellite sensors (e.g., Shi and Xu, 2019).

Finally, the information provided by SITS can be complemented by field-based measurements such as in-field spectral/radiometric readings, and UAV-based aerial surveys, following robust sampling designs. Although obtaining these kinds of data can sometimes present challenges (e.g., high costs or access constraints), it could be crucial for validation purposes. Additionally, information such as management and restoration operations, or other human activities that may influence post-fire ecosystem processes, is usually not easy to obtain remotely.

4.2.3. General applicability and potential methodological improvements

In this study, we showcased the added value of the proposed multi-indicator approach for obtaining thorough diagnostics of changes in ecosystem functioning after wildfire disturbances. Furthermore, our results for the NW-IP highlighted the importance considering both different timeframes of post-fire trajectories, and different dimensions of ecosystem functioning, for characterizing the main patterns of post-fire resilience. Moreover, despite our work using the NW-IP, as a specific study area for illustration purposes, the proposed generic approach can likely be applied to a diverse set of environmental and geographical contexts.

The proposed approach is highly dependent on time-series decomposition procedures to remove the seasonal variation from post-fire trajectories, for the successful extraction of metrics. In this regard, different time-series decomposition strategies could be employed to support the characterization of overall patterns and trends, including break-point detection techniques such as BFAST (Verbesselt et al., 2010a, 2010b). However, these methods target generic change detection through time-series segmentation, rather than specifically characterizing aspects of post-fire trajectories extracted from multiple SITS with diverse features. Furthermore, time-series decomposition procedures could be optimized by automating the selection of its parameter values. Nevertheless, it is important to note that the proposed approach does not address changes in timing or cyclic patterns (e.g., phenology).

Metrics other than the ones proposed in this study could be extracted

from post-fire trajectories for even more enhanced descriptions of post-fire processes. For instance, the value of the trend component at the inflection point could be used as a complementary indicator of fire severity — a more conservative one than the "S95" metric —, by providing estimates of the maximum impact of the wildfire disturbance immediately after a fire. Moreover, the potential of metrics such as "DIT", "RRT" and "RET" as early-warning signals of regime shifts — or even imminent ecosystem collapse —, should be further explored, since critical slowing down implies decreasing post-fire recovery speeds as a system approaches a tipping point (Scheffer et al., 2015; Verbesselt et al., 2016).

Regarding the analysis of post-fire trajectories of albedo, specifically, through spectral indices such as TCTB, extracting two separate sets of metrics — targeting both "darkening" and "brightening" effects separately — could contribute to clarifying the observed post-fire processes in this dimension of ecosystem functioning (Marcos et al., 2021; Quintano et al., 2019; Ramanathan and Carmichael, 2008).

Finally, it must be noted that using the procedures described in the present paper, it is possible that, for some post-fire trajectories, no t_{EQ} will be found — translating into no stable state being reached — within the analyzed period. In our illustrative case, this was observed for a very small portion of the post-fire trajectories, with the highest percentage being ca. 2%, found for TCTB (i.e., albedo). These types of outcomes, which can theoretically translate into incomplete recovery processes, may result from at least one of the following factors: (i) additional wildfire disturbances further in the time series that may prevent the successful detection of the t_{EQ} dates; (ii) seasonal effects may still be present in the time-series, after time-series decomposition, due to sub-optimal seasonal adjustment since seasonal oscillation patterns can change between the pre- and post-fire periods. Additionally, it cannot be excluded that post-fire trajectories may sometimes be exhibiting early-warning signals of imminent regime shifts or even ecosystem collapse, such as "flickering" (i.e., increased variance), which has previously been related to potential critical transitions (Dakos et al., 2012).

5. Conclusions

In this study, we propose an approach for characterizing the resilience of ecosystem functioning to wildfire disturbances by using indicators of resistance and recovery derived from metrics extracted from satellite image time series. These metrics characterize post-fire trajectories in four key dimensions of ecosystem functioning related to the carbon, water, and energy exchanges: (i) vegetation primary production, (ii) vegetation and soil water content, (iii) land surface albedo, and (iv) land surface sensible heat. To showcase our proposed approach, we used MODIS data between 2000 and 2018 to characterize ecosystem resilience to the wildfires that occurred in 2005 in NW Iberian Peninsula. Our approach allowed us to analyze the main patterns of both the effects of and the responses to wildfire disturbances, across the four dimensions of ecosystem functioning considered. Overall, our results suggest that the proposed metrics can successfully depict key features of the post-fire processes in ecosystem functioning, at different timeframes, with a high degree of complementarity among each other, and especially among the different dimensions of ecosystem functioning. This is the main added value of a multi-dimensional approach to analyze ecosystem resilience to wildfire disturbances. We argue that such functional approaches can provide an enhanced characterization of ecosystem resilience to wildfires, ultimately upholding potential implications for post-fire ecosystem management, such as those related with fuel management, planning of biodiversity conservation measures, and prioritization of afforestation and restoration operations.

Supplementary data to this article can be found online at https://doi.org/10.1016/j.rse.2022.113441.

Author contributions

Conceptualization — B.M. with the assistance of J.G., M.C., D.A.S. and J.P.H.; Methodology — B.M. with the assistance of J.G.; Formal analysis — B.M.; Data curation — B.M.; Writing - original draft — B.M. with the assistance of J.G., M.C., D.A.S. and J.P.H.; Writing - review & editing — B.M., J.G., M.C., D.A.S. and J.P.H. All authors have read and agreed to the published version of the manuscript.

Declaration of Competing Interest

The authors declare that they have no known competing financial interests or personal relationships that could have appeared to influence the work reported in this paper.

Data availability

Data will be made available on request.

Acknowledgments

This research was supported by Portuguese national funds through FCT—Foundation for Science and Technology, I.P., under the SeverusPT project (PCIF/RPG/0170/2019). B.M. was supported by the Ministry of Education and Science, and the European Social Fund, within the 2014–2020 EU Strategic Framework, through FCT (PhD scholarship SFRH/BD/99469/2014). J.G. was funded by the Individual Scientific Employment Stimulus Program (2017), through FCT (contract nr. CEECIND/02331/2017). D.A.S. was supported by the projects LifeWatch-2019-10-UGR-01 funded by Ministerio de Ciencia e Innovación/Universidad de Granada/FEDER, and RESISTE (P18-RT-1927) funded by Consejería de Economía, Conocimiento y Universidad from Junta de Andalucía/FEDER.

We acknowledge the use of MODIS imagery obtained from NASA's Land Processes Distributed Active Archive Center (LP DAAC), available at no charge.

References

Adámek, M., Hadincová, V., Wild, J., 2016. Long-term effect of wildfires on temperate Pinus sylvestris forests: vegetation dynamics and ecosystem resilience. For. Ecol. Manag. 380, 285–295. https://doi.org/10.1016/j.foreco.2016.08.051.

Alcaraz-Segura, D., Cabello, J., Paruelo, J.M., Delibes, M., 2008. Trends in the surface vegetation dynamics of the national parks of Spain as observed by satellite sensors. Appl. Veg. Sci. 11, 431–440. https://doi.org/10.3170/2008-7-18522.

Andersen, T., Carstensen, J., Hernández-García, E., Duarte, C.M., 2009. Ecological thresholds and regime shifts: approaches to identification. Trends Ecol. Evol. 24, 49–57. https://doi.org/10.1016/j.tree.2008.07.014.

Arnan, X., Rodrigo, A., Retana, J., 2007. Post-fire regeneration of Mediterranean plant communities at a regional scale is dependent on vegetation type and dryness. J. Veg. Sci. 18, 111–122. https://doi.org/10.1111/j.1654-1103.2007.tb02521.x.

Baho, D.L., Allen, C.R., Garmestani, A., Fried-Petersen, H., Renes, S.E., Gunderson, L., Angeler, D.G., 2017. A quantitative framework for assessing ecological resilience. Ecol. Soc. 22, 1. https://doi.org/10.5751/ES-09427-220317.

Bastos, A., Gouveia, C.M., DaCamara, C.C., Trigo, R.M., 2011. Modelling post-fire vegetation recovery in Portugal. Biogeosciences 8, 3593–3607. https://doi.org/10.5194/bg-8-3593-2011.

Beringer, J., Hutley, L.B., Tapper, N.J., Coutts, A., Kerley, A., O'Grady, A.P., 2003. Fire impacts on surface heat, moisture and carbon fluxes from a tropical savanna in northern Australia. Int. J. Wildland Fire 12, 333–340. https://doi.org/10.1071/wf03023.

Bisson, M., Fornaciai, A., Coli, A., Mazzarini, F., Pareschi, M.T., 2008. The vegetation resilience after fire (VRAF) index: development, implementation and an illustration from Central Italy. Int. J. Appl. Earth Obs. Geoinf. 10, 312–329. https://doi.org/10.1016/j.jag.2007.12.003.

Bodí, M.B., Martin, D.A., Balfour, V.N., Santín, C., Doerr, S.H., Pereira, P., Cerdà, A., Mataix-Solera, J., 2014. Wildland fire ash: production, composition and eco-hydro-geomorphic effects. Earth-Sci. Rev. 130, 103–127. https://doi.org/10.1016/j.earscirev.2013.12.007.

Boettiger, C., Ross, N., Hastings, A., 2013. Early warning signals: the charted and uncharted territories. Theor. Ecol. 6, 255–264. https://doi.org/10.1007/s12080-013-0192-6.

Bowman, D.M.J.S., Balch, J.K., Artaxo, P., Bond, W.J., Carlson, J.M., Cochrane, M.A., D'Antonio, C.M., DeFries, R.S., Doyle, J.C., Harrison, S.P., Johnston, F.H., Keeley, J.

E., Krawchuk, M.A., Kull, C.A., Marston, J.B., Moritz, M.A., Prentice, I.C., Roos, C.I., Scott, A.C., Swetnam, T.W., van der Werf, G.R., Pyne, S.J., 2009. Fire in the earth system. Science 324, 481–484. https://doi.org/10.1126/science.1163886.

Bowman, D.M.J.S., Perry, G.L.W., Marston, J.B., 2015. Feedbacks and landscape-level vegetation dynamics. Trends Ecol. Evol. 30, 255–260. https://doi.org/10.1016/j.tree.2015.03.005.

Busetto, L., Ranghetti, L., 2016. MODIStsp: an R package for automatic preprocessing of MODIS land products time series. Comput. Geosci. 97, 40–48. https://doi.org/10.1016/j.cageo.2016.08.020.

Caccamo, G., Bradstock, R., Collins, L., Penman, T., Watson, P., 2015. Using MODIS data to analyse post-fire vegetation recovery in Australian eucalypt forests. J. Spat. Sci. 60, 341–352. https://doi.org/10.1080/14498596.2015.974227.

Carvalho-Santos, C., Marcos, B., Nunes, J., Regos, A., Palazzi, E., Terzago, S., Monteiro, A., Honrado, J., 2019. Hydrological impacts of large fires and future climate: Modeling approach supported by satellite data. Remote Sens. 11, 2832. https://doi.org/10.3390/rs11232832.

Catry, F.X., Rego, F.C., Bação, F.L., Moreira, F., 2009. Modeling and mapping wildfire ignition risk in Portugal. Int. J. Wildland Fire 18, 921. https://doi.org/10.1071/WF07123.

Chuvieco, E., Mouillot, F., van der Werf, G.R., San Miguel, J., Tanase, M., Koutsias, N., García, M., Yebra, M., Padilla, M., Gitas, I., Heil, A., Hawbaker, T.J., Giglio, L., 2019. Historical background and current developments for mapping burned area from satellite earth observation. Remote Sens. Environ. 225, 45–64. https://doi.org/10.1016/j.rse.2019.02.013.

Cleveland, R.B., Cleveland, W.S., McRae, J.E., Terpenning, I., 1990. STL: a seasonal-trend decomposition procedure based on loess. J. Off. Stat. 6, 3–73.

Coop, J.D., Parks, S.A., Stevens-Rumann, C.S., Crausbay, S.D., Higuera, P.E., Hurteau, M. D., Tepley, A., Whitman, E., Assal, T., Collins, B.M., Davis, K.T., Dobrowski, S., Falk, D.A., Fornwalt, P.J., Fulé, P.Z., Harvey, B.J., Kane, V.R., Littlefield, C.E., Margolis, E.Q., North, M., Parisien, M.-A., Prichard, S., Rodman, K.C., 2020. Wildfire-driven forest conversion in Western North American landscapes. Bioscience 70, 659–673. https://doi.org/10.1093/biosci/biaa061.

Coops, N.C., Wulder, M.A., Duro, D.C., Han, T., Berry, S., 2008. The development of a Canadian dynamic habitat index using multi-temporal satellite estimates of canopy light absorbance. Ecol. Indic. 8, 754–766. https://doi.org/10.1016/j.ecolind.2008.01.007.

Cui, X., Gibbes, C., Southworth, J., Waylen, P., 2013. Using remote sensing to quantify vegetation change and ecological resilience in a semi-arid system. Land 2, 108–130. https://doi.org/10.3390/land2020108.

Dakos, V., Carpenter, S.R., Brock, W.A., Ellison, A.M., Guttal, V., Ives, A.R., Kéfi, S., Livina, V., Seekell, D.A., van Nes, E.H., Scheffer, M., 2012. Methods for detecting early warnings of critical transitions in time series illustrated using simulated ecological data. PLoS One 7, e41010. https://doi.org/10.1371/journal.pone.0041010.

Day, N.J., White, A.L., Johnstone, J.F., Degré-Timmons, G.É., Cumming, S.G., Mack, M. C., Turetsky, M.R., Walker, X.J., Baltzer, J.L., 2020. Fire characteristics and environmental conditions shape plant communities via regeneration strategy. Ecography (Cop.) 43, 1464–1474. https://doi.org/10.1111/ecog.05211.

De Keersmaecker, W., Lhermitte, S., Tits, L., Honnay, O., Somers, B., Coppin, P., 2015. A model quantifying global vegetation resistance and resilience to short-term climate anomalies and their relationship with vegetation cover. Glob. Ecol. Biogeogr. 24, 539–548. https://doi.org/10.1111/geb.12279.

Delettre, O., 2021. Identity of ecological systems and the meaning of resilience. J. Ecol. 1365-2745, 13655. https://doi.org/10.1111/1365-2745.13655.

Di Mauro, B., Fava, F., Busetto, L., Crosta, G.F., Colombo, R., 2014. Post-fire resilience in the alpine region estimated from MODIS satellite multispectral data. Int. J. Appl. Earth Obs. Geoinf. 32, 163–172. https://doi.org/10.1016/j.jag.2014.04.010.

Díaz-Delgado, R., Lloret, F., Pons, X., Terradas, J., 2002. Satellite evidence of decreasing resilience in Mediterranean plant communities after recurrent wildfires. Ecology 83, 2293–2303. https://doi.org/10.1890/0012-9658(2002)083[2293:SEODRI]2.0.CO;2.

Donohue, I., Petchey, O.L., Montoya, J.M., Jackson, A.L., McNally, L., Viana, M., Healy, K., Lurgi, M., O'Connor, N.E., Emmerson, M.C., 2013. On the dimensionality of ecological stability. Ecol. Lett. 16, 421–429. https://doi.org/10.1111/ele.12086.

Donohue, I., Hillebrand, H., Montoya, J.M., Petchey, O.L., Pimm, S.L., Fowler, M.S., Healy, K., Jackson, A.L., Lurgi, M., McClean, D., O'Connor, N.E., O'Gorman, E.J., Yang, Q., 2016. Navigating the complexity of ecological stability. Ecol. Lett. 19, 1172–1185. https://doi.org/10.1111/ele.12648.

Duan, S.-B., Li, Z.-L., Li, H., Göttsche, F.-M., Wu, H., Zhao, W., Leng, P., Zhang, X., Coll, C., 2019. Validation of collection 6 MODIS land surface temperature product using in situ measurements. Remote Sens. Environ. 225, 16–29. https://doi.org/10.1016/j.rse.2019.02.020.

Dwomoh, F.K., Wimberly, M.C., 2017. Fire regimes and forest resilience: alternative vegetation states in the west African tropics. Landsc. Ecol. 32, 1849–1865. https://doi.org/10.1007/s10980-017-0553-4.

Ebel, B.A., Martin, D.A., 2017. Meta-analysis of field-saturated hydraulic conductivity recovery following wildland fire: applications for hydrologic model parameterization and resilience assessment. Hydrol. Process. 31, 3682–3696. https://doi.org/10.1002/HYP.11288.

Elmqvist, T., Folke, C., Nystrom, M., Peterson, G., Bengtsson, J., Walker, B., Norberg, J., 2003. Response diversity, ecosystem change, and resilience. Front. Ecol. Environ. 1, 488. https://doi.org/10.2307/3868116.

Falk, D.A., 2017. Restoration ecology, resilience, and the axes of change 1, 102, pp. 201–216. https://doi.org/10.3417/2017006.

Falk, D.A., Watts, A.C., Thode, A.E., 2019. Scaling ecological resilience. Front. Ecol. Evol. 7, 275. https://doi.org/10.3389/FEVO.2019.00275/BIBTEX.

Falk, D.A., van Mantgem, P.J., Keeley, J.E., Gregg, R.M., Guiterman, C.H., Tepley, A.J., Young, J.N., Marshall, L.A., 2022. Mechanisms of forest resilience. For. Ecol. Manag. 512, 120129 https://doi.org/10.1016/j.foreco.2022.120129.

Fan, X., Hao, X., Hao, H., Zhang, J., Li, Y., 2021. Comprehensive assessment Indicator of ecosystem resilience in Central Asia. Water 13, 124. https://doi.org/10.3390/w13020124.

Fernandez-Manso, A., Quintano, C., Roberts, D.A., 2016. Burn severity influence on post-fire vegetation cover resilience from Landsat MESMA fraction images time series in Mediterranean forest ecosystems. Remote Sens. Environ. 184, 112–123. https://doi.org/10.1016/j.rse.2016.06.015.

Folke, C., Carpenter, S., Walker, B., Scheffer, M., Elmqvist, T., Gunderson, L., Holling, C. S., 2004. Regime shifts, resilience, and biodiversity in ecosystem management. Annu. Rev. Ecol. Evol. Syst. 35, 557–581. https://doi.org/10.1146/annurev.ecolsys.35.021103.105711.

Frazier, A.E., Renschler, C.S., Miles, S.B., 2013. Evaluating post-disaster ecosystem resilience using MODIS GPP data. Int. J. Appl. Earth Obs. Geoinf. 21, 43–52. https://doi.org/10.1016/j.jag.2012.07.019.

French, N.H.F., Whitley, M.A., Jenkins, L.K., 2016. Fire disturbance effects on land surface albedo in Alaskan tundra. J. Geophys. Res. Biogeosci. 121, 841–854. https://doi.org/10.1002/2015JG003177.

García-Llamas, P., Suárez-Seoane, S., Fernández-Guisuraga, J.M., Fernández-García, V., Fernández-Manso, A., Quintano, C., Taboada, A., Marcos, E., Calvo, L., 2019. Evaluation and comparison of Landsat 8, Sentinel-2 and Deimos-1 remote sensing indices for assessing burn severity in Mediterranean fire-prone ecosystems. Int. J. Appl. Earth Obs. Geoinf. 80, 137–144. https://doi.org/10.1016/j.jag.2019.04.006.

Gatebe, C.K.K., Ichoku, C.M.M., Poudyal, R., Román, M.O.O., Wilcox, E., 2014. Surface albedo darkening from wildfires in northern sub-Saharan Africa. Environ. Res. Lett. 9, 065003 https://doi.org/10.1088/1748-9326/9/6/065003.

Giglio, L., Boschetti, L., Roy, D.P., Humber, M.L., Justice, C.O., 2018. The collection 6 MODIS burned area mapping algorithm and product. Remote Sens. Environ. 217, 72–85. https://doi.org/10.1016/j.rse.2018.08.005.

Gillies, S., Ward, B., Petersen, A.S., 2013. Rasterio: geospatial raster I/O for Python programmers version 0.36.0.

Gouveia, C., DaCamara, C.C., Trigo, R.M., 2010. Post-fire vegetation recovery in Portugal based on spot/vegetation data. Nat. Hazards Earth Syst. Sci. 10, 673–684. https://doi.org/10.5194/nhess-10-673-2010.

Gunderson, L.H., 2000. Ecological resilience—in theory and application. Annu. Rev. Ecol. Syst. 31, 425–439. https://doi.org/10.1146/annurev.ecolsys.31.1.425.

Hampel, F.R., 1971. A general qualitative definition of robustness. Ann. Math. Stat. 42, 1887–1896.

Hampel, F.R., 1974. The influence curve and its role in robust estimation. J. Am. Stat. Assoc. 69, 383–393. https://doi.org/10.1080/01621459.1974.10482962.

Hansen, M.J., Franklin, S.E., Woudsma, C., Peterson, M., 2001. Forest structure classification in the North Columbia mountains using the Landsat TM Tasseled cap wetness component. Can. J. Remote. Sens. 27, 20–32. https://doi.org/10.1080/07038992.2001.10854916.

Harris, A., Carr, A.S.S., Dash, J., 2014. Remote sensing of vegetation cover dynamics and resilience across southern Africa. Int. J. Appl. Earth Obs. Geoinf. 28, 131–139. https://doi.org/10.1016/j.jag.2013.11.014.

Healey, S., Cohen, W., Zhiqiang, Y., Krankina, O., 2005. Comparison of Tasseled cap-based Landsat data structures for use in forest disturbance detection. Remote Sens. Environ. 97 (3), 301–310. https://doi.org/10.1016/j.rse.2005.05.009.

Hijmans, R.J., 2020. Raster: Geographic Data Analysis and Modeling. R package version 3.4–5.

Hirota, M., Holmgren, M., Van Nes, E.H., Scheffer, M., 2011. Global resilience of tropical forest and savanna to critical transitions. Science 334, 232–235. https://doi.org/10.1126/science.1210657.

Hodgson, D., McDonald, J.L., Hosken, D.J., 2015. What do you mean, 'resilient'? Trends Ecol. Evol. 30, 503–506. https://doi.org/10.1016/j.tree.2015.06.010.

Holling, C.S., 1973. Resilience and stability of ecological systems. Annu. Rev. Ecol. Syst. 4, 1–23. https://doi.org/10.1146/annurev.es.04.110173.000245.

Holling, C.S., 1996. Engineering resilience versus ecological resilience. In: Schulze, P.E. (Ed.), Engineering within Ecological Constraints. National Academies Press, Washington, D.C, pp. 31–43. https://doi.org/10.17226/4919.

Hope, A., Tague, C., Clark, R., 2007. Characterizing post-fire vegetation recovery of California chaparral using TM/ETM+ time-series data. Int. J. Remote Sens. 28, 1339–1354. https://doi.org/10.1080/01431160600908924.

Hope, A., Albers, N., Bart, R., 2012. Characterizing post-fire recovery of fynbos vegetation in the Western cape region of South Africa using MODIS data. Int. J. Remote Sens. 33, 979–999. https://doi.org/10.1080/01431161.2010.543184.

Hubbert, K.R., Wohlgemuth, P.M., Beyers, J.L., Narog, M.G., Gerrard, R., 2012. Post-fire soil water repellency, hydrologic response, and sediment yield compared between grass-converted and chaparral watersheds. Fire Ecol. 8, 143–162. https://doi.org/10.4996/fireecology.0802143.

Hyndman, R.J., Athanasopoulos, G., 2018. Forecasting: Principles and Practice, 2nd ed. OTexts, Melbourne, Australia.

Ingrisch, J., Bahn, M., 2018. Towards a comparable quantification of resilience. Trends Ecol. Evol. 33, 251–259. https://doi.org/10.1016/j.tree.2018.01.013.

João, T., João, G., Bruno, M., João, H., 2018. Indicator-based assessment of post-fire recovery dynamics using satellite NDVI time-series. Ecol. Indic. 89, 199–212. https://doi.org/10.1016/j.ecolind.2018.02.008.

Johnstone, J.F., Chapin, F.S., Hollingsworth, T.N., Mack, M.C., Romanovsky, V., Turetsky, M., 2010. Fire, climate change, and forest resilience in interior alaska1. Can. J. For. Res. 40, 1302–1312. https://doi.org/10.1139/X10-061.

Keeley, J.E., 2009. Fire intensity, fire severity and burn severity: a brief review and suggested usage. Int. J. Wildland Fire 18, 116. https://doi.org/10.1071/WF07049.

Kitzberger, T., Falk, D.A., Westerling, A.L., Swetnam, T.W., 2017. Direct and indirect climate controls predict heterogeneous early-mid 21st century wildfire burned area across western and boreal North America. PLoS One 12, e0188486. https://doi.org/10.1371/journal.pone.0188486.

Kolden, C.A., Lutz, J.A., Key, C.H., Kane, J.T., van Wagtendonk, J.W., 2012. Mapped versus actual burned area within wildfire perimeters: characterizing the unburned. For. Ecol. Manag. 286, 38–47. https://doi.org/10.1016/j.foreco.2012.08.020.

van Leeuwen, W.J.D., Casady, G.M., Neary, D.G., Bautista, S., Alloza, J.A., Carmel, Y., Wittenberg, L., Malkinson, D., Orr, B.J., 2010. Monitoring post-wildfire vegetation response with remotely sensed time-series data in Spain, USA and Israel. Int. J. Wildland Fire 19, 75. https://doi.org/10.1071/WF08078.

Lentile, L.B., Holden, Z.A., Smith, A.M.S.S., Falkowski, M.J., Hudak, A.T., Morgan, P., Lewis, S.A., Gessler, P.E., Benson, N.C., Lentile, L.B., Holden, Z.A., Smith, A.M.S.S., Falkowski, M.J., Hudak, A.T., Morgan, P., Lewis, S.A., Gessler, P.E., Benson, N.C., 2006. Remote sensing techniques to assess active fire characteristics and post-fire effects. Int. J. Wildland Fire 15, 319. https://doi.org/10.1071/WF05097.

Leys, B., Higuera, P.E., McLauchlan, K.K., Dunnette, P.V., 2016. Wildfires and geochemical change in a subalpine forest over the past six millennia. Environ. Res. Lett. 11, 125003 https://doi.org/10.1088/1748-9326/11/12/125003.

Liu, Z., Ballantyne, A.P., Cooper, L.A., 2018a. Increases in land surface temperature in response to fire in Siberian boreal forests and their attribution to biophysical processes. Geophys. Res. Lett. 45, 6485–6494. https://doi.org/10.1029/2018GL078283.

Liu, H., Zhan, Q., Yang, C., Wang, J., 2018b. Characterizing the Spatio-temporal pattern of land surface temperature through time series clustering: based on the latent pattern and morphology. Remote Sens. 10, 654. https://doi.org/10.3390/rs10040654.

Liu, Z., Ballantyne, A.P., Cooper, L.A., 2019. Biophysical feedback of global forest fires on surface temperature. Nat. Commun. 10, 1–9. https://doi.org/10.1038/s41467-018-08237-z.

Liu, F., Liu, H., Xu, C., Shi, L., Zhu, X., Qi, Y., He, W., 2021. Old-growth forests show low canopy resilience to droughts at the southern edge of the taiga. Glob. Chang. Biol. 27, 2392–2402. https://doi.org/10.1111/gcb.15605.

Lobser, S.E., Cohen, W.B., 2007. MODIS tasselled cap: land cover characteristics expressed through transformed MODIS data. Int. J. Remote Sens. 28, 5079–5101. https://doi.org/10.1080/01431160701253303.

MacDonald, L.H., Huffman, E.L., 2004. Post-fire soil water repellency. Soil Sci. Soc. Am. J. 68, 1729–1734. https://doi.org/10.2136/sssaj2004.1729.

Maffei, C., Alfieri, S.M., Menenti, M., 2018. Relating spatiotemporal patterns of Forest fires burned area and duration to diurnal land surface temperature anomalies. Remote Sens. 10, 1777. https://doi.org/10.3390/rs10111777.

Marcos, E., Fernández-García, V., Fernández-Manso, A., Quintano, C., Valbuena, L., Tárrega, R., Luis-Calabuig, E., Calvo, L., 2018. Evaluation of composite burn index and land surface temperature for assessing soil burn severity in Mediterranean fire-prone pine ecosystems. Forests 9, 494. https://doi.org/10.3390/f9080494.

Marcos, B., Gonçalves, J., Alcaraz-Segura, D., Cunha, M., Honrado, J.P., 2019. Improving the detection of wildfire disturbances in space and time based on indicators extracted from MODIS data: a case study in northern Portugal. Int. J. Appl. Earth Obs. Geoinf. 78, 77–85. https://doi.org/10.1016/j.jag.2018.12.003.

Marcos, B., Gonçalves, J., Alcaraz-Segura, D., Cunha, M., Honrado, J.P., 2021. A framework for multi-dimensional assessment of wildfire disturbance severity from remotely sensed ecosystem functioning attributes. Remote Sens. 13, 780. https://doi.org/10.3390/rs13040780.

McGuire, L.A., Youberg, A.M., 2019. Impacts of successive wildfire on soil hydraulic properties: implications for debris flow hazards and system resilience. Earth Surf. Process. Landf. 44, 2236–2250. https://doi.org/10.1002/ESP.4632.

Meddens, A.J.H., Kolden, C.A., Lutz, J.A., Abatzoglou, J.T., Hudak, A.T., 2018. Spatiotemporal patterns of unburned areas within fire perimeters in the northwestern United States from 1984 to 2014. Ecosphere 9, e02029. https://doi.org/10.1002/ecs2.2029.

Meng, R., Wu, J., Zhao, F., Cook, B.D., Hanavan, R.P., Serbin, S.P., 2018. Measuring short-term post-fire forest recovery across a burn severity gradient in a mixed pine-oak forest using multi-sensor remote sensing techniques. Remote Sens. Environ. 210, 282–296. https://doi.org/10.1016/J.RSE.2018.03.019.

Meng, J.-N., Fang, H., Scavia, D., 2021. Application of ecosystem stability and regime shift theories in ecosystem assessment-calculation variable and practical performance. Ecol. Indic. 125, 107529 https://doi.org/10.1016/j.ecolind.2021.107529.

Mildrexler, D.J., Zhao, M., Running, S.W., 2009. Testing a MODIS global disturbance index across North America. Remote Sens. Environ. 113, 2103–2117. https://doi.org/10.1016/j.rse.2009.05.016.

Millar, C.I., Stephenson, N.L., Stephens, S.L., 2007. Climate change and forests of the future: managing in the face of uncertainty. Ecol. Appl. 17, 2145–2151. https://doi.org/10.1890/06-1715.1.

Moreira, F., Ascoli, D., Safford, H., Adams, M.A., Moreno, J.M., Pereira, J.M.C., Catry, F. X., Armesto, J., Bond, W., González, M.E., Curt, T., Koutsias, N., McCaw, L., Price, O., Pausas, J.G., Rigolot, E., Stephens, S., Tavsanoglu, C., Vallejo, V.R., Van Wilgen, B. W., Xanthopoulos, G., Fernandes, P.M., 2020. Wildfire management in Mediterranean-type regions: paradigm change needed. Environ. Res. Lett. 15, 011001 https://doi.org/10.1088/1748-9326/ab541e.

Mouillot, F., Schultz, M.G., Yue, C., Cadule, P., Tansey, K., Ciais, P., Chuvieco, E., 2014. Ten years of global burned area products from spaceborne remote sensing—a review: analysis of user needs and recommendations for future developments. Int. J. Appl. Earth Obs. Geoinf. 26, 64–79. https://doi.org/10.1016/j.jag.2013.05.014.

Nguyen, T.H., Jones, S.D., Soto-Berelov, M., Haywood, A., Hislop, S., 2018. A spatial and temporal analysis of forest dynamics using Landsat time-series. Remote Sens. Environ. 217, 461–475. https://doi.org/10.1016/J.RSE.2018.08.028.

North, M.P., Stevens, J.T., Greene, D.F., Coppoletta, M., Knapp, E.E., Latimer, A.M., Restaino, C.M., Tompkins, R.E., Welch, K.R., York, R.A., Young, D.J.N., Axelson, J. N., Buckley, T.N., Estes, B.L., Hager, R.N., Long, J.W., Meyer, M.D., Ostoja, S.M., Safford, H.D., Shive, K.L., Tubbesing, C.L., Vice, H., Walsh, D., Werner, C.M., Wyrsch, P., 2019. Tamm review: reforestation for resilience in dry western U.S. forests. For. Ecol. Manag. 432, 209–224. https://doi.org/10.1016/J.FORECO.2018.09.007.

Oliveira, S.L.J., Pereira, J.M.C., Carreiras, J.M.B., Abaimov, S., Turcotte, D., Shcherbakov, R., Rundle, J., Díaz-Delgado, R., Lloret, F., Pons, X., Fisher, J., Loneragan, W., Dixon, K., Delaney, J., Veneklaas, E., Grissino-Mayer, H., Heinselman, M., Johnson, E., Gutsell, S., Kraaij, T., Lloret, F., Marí, G., McCarthy, M., Gill, A., Bradstock, R., Moritz, M., Moritz, M., Keeley, J., Johnson, E., Shaffner, A., Moritz, M., Moody, T., Miles, L., Smith, M., Valpine, P., Nunes, M., Vasconcelos, M., Pereira, J., Dasgupta, N., Alldredge, R., Rego, F., O'Donnell, A., Boer, M., McCaw, W., Grierson, P., Pereira, M., Trigo, R., DaCamara, C., Pereira, J., Leite, S., Polakow, D., Dunne, T., Trigo, R., Pereira, J., Pereira, M., Mota, B., Calado, T., DaCamara, C., Santo, F., Vázquez, A., Moreno, J., 2012. Fire frequency analysis in Portugal (1975–2005), using Landsat-based burnt area maps. Int. J. Wildland Fire 21, 48. https://doi.org/10.1071/WF10131.

Parks, S.A., Holsinger, L.M., Koontz, M.J., Collins, L., Whitman, E., Parisien, M.-A., Loehman, R.A., Barnes, J.L., Bourdon, J.-F., Boucher, J., Boucher, Y., Caprio, A.C., Collingwood, A., Hall, R.J., Park, J., Saperstein, L.B., Smetanka, C., Smith, R.J., Soverel, N., 2019. Giving ecological meaning to satellite-derived fire severity metrics across North American forests. Remote Sens. 11, 1735. https://doi.org/10.3390/rs11141735.

Parra, A., Moreno, J.M., 2018. Drought differentially affects the post-fire dynamics of seeders and resprouters in a Mediterranean shrubland. Sci. Total Environ. 626, 1219–1229. https://doi.org/10.1016/j.scitotenv.2018.01.174.

Pausas, J.G., Paula, S., 2012. Fuel shapes the fire-climate relationship: evidence from Mediterranean ecosystems. Glob. Ecol. Biogeogr. 21, 1074–1082. https://doi.org/10.1111/j.1466-8238.2012.00769.x.

Pellegrini, A.F.A., Ahlström, A., Hobbie, S.E., Reich, P.B., Nieradzik, L.P., Staver, A.C., Scharenbroch, B.C., Jumpponen, A., Anderegg, W.R.L., Randerson, J.T., Jackson, R. B., 2018. Fire frequency drives decadal changes in soil carbon and nitrogen and ecosystem production. Nature 553, 194–198. https://doi.org/10.1038/nature24668.

Petropoulos, G., Carlson, T.N., Wooster, M.J., Islam, S., 2009. A review of Ts/VI remote sensing based methods for the retrieval of land surface energy fluxes and soil surface moisture. Prog. Phys. Geogr. 33, 224–250. https://doi.org/10.1177/0309133309338997.

Prior, L.D., Bowman, D.M.J.S., 2020. Classification of post-fire responses of Woody plants to include Pyrophobic communities. Fire 3, 15. https://doi.org/10.3390/fire3020015.

Prodon, R., Diaz-Delgado, R., 2021. Assessing the postfire resilience of a Mediterranean forest from satellite and ground data (NDVI, vegetation profile, avifauna). Écoscience 1–11. https://doi.org/10.1080/11956860.2021.1871826.

Quintano, C., Fernández-Manso, A., Calvo, L., Marcos, E., Valbuena, L., 2015. Land surface temperature as potential indicator of burn severity in forest Mediterranean ecosystems. Int. J. Appl. Earth Obs. Geoinf. 36, 1–12. https://doi.org/10.1016/j.jag.2014.10.015.

Quintano, C., Fernandez-Manso, A., Marcos, E., Calvo, L., 2019. Burn severity and post-fire land surface albedo relationship in Mediterranean Forest ecosystems. Remote Sens. 11, 2309. https://doi.org/10.3390/rs11192309.

R Core Team, 2021. R: A Language and Environment for Statistical Computing version 4.0.4.

Ramanathan, V., Carmichael, G., 2008. Global and regional climate changes due to black carbon. Nat. Geosci. 1, 221–227. https://doi.org/10.1038/ngeo156.

Roy, D.P., Huang, H., Boschetti, L., Giglio, L., Yan, L., Zhang, H.H., Li, Z., 2019. Landsat-8 and Sentinel-2 burned area mapping - a combined sensor multi-temporal change detection approach. Remote Sens. Environ. 231, 111254 https://doi.org/10.1016/j.rse.2019.111254.

Ryu, J.-H., Han, K.-S., Hong, S., Park, N.-W., Lee, Y.-W., Cho, J., 2018. Satellite-Based Evaluation of the Post-Fire Recovery Process from the Worst Forest Fire Case in South Korea, 10, p. 918.

Saha, M.V., D'Odorico, P., Scanlon, T.M., 2017. Albedo changes after fire as an explanation of fire-induced rainfall suppression. Geophys. Res. Lett. 44, 3916–3923. https://doi.org/10.1002/2017GL073623.

Saha, M.V., D'Odorico, P., Scanlon, T.M., 2019. Kalahari wildfires drive continental post-fire brightening in sub-Saharan Africa. Remote Sens. 11, 1090. https://doi.org/10.3390/rs11091090.

Samiappan, S., Hathcock, L., Turnage, G., McCraine, C., Pitchford, J., Moorhead, R., 2019. Remote sensing of wildfire using a small unmanned aerial system: post-fire mapping, vegetation recovery and damage analysis in Grand Bay, Mississippi/Alabama, USA. Drones 3, 43. https://doi.org/10.3390/drones3020043.

San-Miguel-Ayanz, J., Moreno, J.M., Camia, A., 2013. Analysis of large fires in European Mediterranean landscapes: lessons learned and perspectives. For. Ecol. Manag. 294, 11–22. https://doi.org/10.1016/j.foreco.2012.10.050.

Santos, R.M.B., Sanches Fernandes, L.F., Pereira, M.G., Cortes, R.M.V., Pacheco, F.A.L., 2015. Water resources planning for a river basin with recurrent wildfires. Sci. Total Environ. 526, 1–13. https://doi.org/10.1016/j.scitotenv.2015.04.058.

Scheffer, M., Carpenter, S.R., 2003. Catastrophic regime shifts in ecosystems: linking theory to observation. Trends Ecol. Evol. 18, 648–656. https://doi.org/10.1016/j.tree.2003.09.002.

Scheffer, M., Bascompte, J., Brock, W.A., Brovkin, V., Carpenter, S.R., Dakos, V., Held, H., van Nes, E.H., Rietkerk, M., Sugihara, G., 2009. Early-warning signals for critical transitions. Nature 461, 53–59. https://doi.org/10.1038/nature08227.

Scheffer, M., Carpenter, S.R., Lenton, T.M., Bascompte, J., Brock, W., Dakos, V., van de Koppel, J., van de Leemput, I.A., Levin, S.A., van Nes, E.H., Pascual, M., Vandermeer, J., 2012. Anticipating critical transitions. Science 80). 338, 344–348. https://doi.org/10.1126/science.1225244.

Scheffer, M., Carpenter, S.R., Dakos, V., van Nes, E.H., 2015. Generic indicators of ecological resilience: inferring the chance of a critical transition. Annu. Rev. Ecol. Evol. Syst. 46, 145–167. https://doi.org/10.1146/annurev-ecolsys-112414-054242.

Selles, O.A., Rissman, A.R., 2020. Content analysis of resilience in forest fire science and management. Land Use Policy 94, 104483. https://doi.org/10.1016/j.landusepol.2020.104483.

Semeraro, T., Vacchiano, G., Aretano, R., Ascoli, D., 2019. Application of vegetation index time series to value fire effect on primary production in a southern European rare wetland. Ecol. Eng. 134, 9–17. https://doi.org/10.1016/j.ecoleng.2019.04.004.

Senf, C., Seidl, R., 2020. Mapping the forest disturbance regimes of Europe. Nat. Sustain. 4 https://doi.org/10.1038/s41893-020-00609-y.

Shi, T., Xu, H., 2019. Derivation of Tasseled cap transformation coefficients for Sentinel-2 MSI at-sensor reflectance data. IEEE J. Sel. Top. Appl. Earth Obs. Remote Sens. 12, 4038–4048. https://doi.org/10.1109/JSTARS.2019.2938388.

Smith, H.G., Sheridan, G.J., Lane, P.N.J., Nyman, P., Haydon, S., 2011. Wildfire effects on water quality in forest catchments: a review with implications for water supply. J. Hydrol. 396, 170–192. https://doi.org/10.1016/j.jhydrol.2010.10.043.

Smith, A.M.S.S., Kolden, C.A., Tinkham, W.T., Talhelm, A.F., Marshall, J.D., Hudak, A.T., Boschetti, L., Falkowski, M.J., Greenberg, J.A., Anderson, J.W., Kliskey, A., Alessa, L., Keefe, R.F., Gosz, J.R., 2014. Remote sensing the vulnerability of vegetation in natural terrestrial ecosystems. Remote Sens. Environ. 154, 322–337. https://doi.org/10.1016/j.rse.2014.03.038.

Sparks, A.M., Kolden, C.A., Smith, A.M.S., Boschetti, L., Johnson, D.M., Cochrane, M.A., 2018. Fire intensity impacts on post-fire temperate coniferous forest net primary production. Biogeosciences 15, 1173–1183. https://doi.org/10.5194/bg-15-1173-2018.

Spasojevic, M.J., Bahlai, C.A., Bradley, B.A., Butterfield, B.J., Tuanmu, M.-N., Sistla, S., Wiederholt, R., Suding, K.N., 2016. Scaling up the diversity-resilience relationship with trait databases and remote sensing data: the recovery of production after wildfire. Glob. Chang. Biol. 22, 1421–1432. https://doi.org/10.1111/gcb.13174.

Staal, A., van Nes, E.H., Hantson, S., Holmgren, M., Dekker, S.C., Pueyo, S., Xu, C., Scheffer, M., 2018. Resilience of tropical tree cover: the roles of climate, fire, and herbivory. Glob. Chang. Biol. 24, 5096–5109. https://doi.org/10.1111/gcb.14408.

Sun, X., Zou, C.B., Wilcox, B., Stebler, E., 2019. Effect of vegetation on the energy balance and evapotranspiration in tallgrass prairie: a paired study using the Eddy-covariance method. Boundary-Layer Meteorol. 170, 127–160. https://doi.org/10.1007/s10546-018-0388-9.

Swetnam, T.L., Yool, S.R., Roy, S., Falk, D.A., 2021. On the use of standardized multi-temporal indices for monitoring disturbance and ecosystem moisture stress across multiple earth observation Systems in the Google Earth Engine. Remote Sens. 13, 1448. https://doi.org/10.3390/rs13081448.

Tedim, F., Remelgado, R., Borges, C., Carvalho, S., Martins, J., 2013. Exploring the occurrence of mega-fires in Portugal. For. Ecol. Manag. 294, 86–96. https://doi.org/10.1016/j.foreco.2012.07.031.

Tiribelli, F., Kitzberger, T., Morales, J.M., 2018. Changes in vegetation structure and fuel characteristics along post-fire succession promote alternative stable states and positive fire-vegetation feedbacks. J. Veg. Sci. 29, 147–156. https://doi.org/10.1111/jvs.12620.

Veraverbeke, S., Lhermitte, S., Verstraeten, W.W., Goossens, R., 2011a. A time-integrated MODIS burn severity assessment using the multi-temporal differenced normalized burn ratio (dNBRMT). Int. J. Appl. Earth Obs. Geoinf. 13, 52–58. https://doi.org/10.1016/j.jag.2010.06.006.

Veraverbeke, S., Lhermitte, S., Verstraeten, W.W., Goossens, R., 2011b. Evaluation of pre/post-fire differenced spectral indices for assessing burn severity in a Mediterranean environment with Landsat thematic mapper. Int. J. Remote Sens. 32, 3521–3537. https://doi.org/10.1080/01431161003752430.

Veraverbeke, S., Gitas, I., Katagis, T., Polychronaki, A., Somers, B., Goossens, R., 2012a. Assessing post-fire vegetation recovery using red–near infrared vegetation indices: accounting for background and vegetation variability. ISPRS J. Photogramm. Remote Sens. 68, 28–39. https://doi.org/10.1016/j.isprsjprs.2011.12.007.

Veraverbeke, S., Verstraeten, W.W., Lhermitte, S., Van De Kerchove, R., Goossens, R., 2012b. Assessment of post-fire changes in land surface temperature and surface albedo, and their relation with fire - burn severity using multitemporal MODIS imagery. Int. J. Wildland Fire 21, 243. https://doi.org/10.1071/WF10075.

Verbesselt, J., Hyndman, R., Newnham, G., Culvenor, D., 2010a. Detecting trend and seasonal changes in satellite image time series. Remote Sens. Environ. 114, 106–115. https://doi.org/10.1016/j.rse.2009.08.014.

Verbesselt, J., Hyndman, R., Zeileis, A., Culvenor, D., 2010b. Phenological change detection while accounting for abrupt and gradual trends in satellite image time series. Remote Sens. Environ. 114, 2970–2980. https://doi.org/10.1016/j.rse.2010.08.003.

Verbesselt, J., Umlauf, N., Hirota, M., Holmgren, M., Van Nes, E.H., Herold, M., Zeileis, A., Scheffer, M., 2016. Remotely sensed resilience of tropical forests. Nat. Clim. Chang. 6, 1028–1031. https://doi.org/10.1038/nclimate3108.

Vermote, E., 2015. MOD09A1 MODIS/Terra Surface Reflectance 8-Day L3 Global 500m SIN Grid V006. NASA EOSDIS L. Process. DAAC.

Viana-Soto, A., Aguado, I., Salas, J., García, M., 2020. Identifying post-fire recovery trajectories and driving factors using landsat time series in fire-prone mediterranean pine forests. Remote Sens. 12, 1499. https://doi.org/10.3390/RS12091499.

Vlassova, L., Pérez-Cabello, F., Mimbrero, M., Llovería, R., García-Martín, A., 2014. Analysis of the relationship between land surface temperature and wildfire severity in a series of Landsat images. Remote Sens. 6, 6136–6162. https://doi.org/10.3390/rs6076136.

Wan, Z., Hook, S., Hulley, G., 2015. MOD11A2 MODIS/Terra Land Surface Temperature/Emissivity 8-Day L3 Global 1km SIN Grid V006. NASA EOSDIS L. Process. DAAC.

Wei, X., Hayes, D.J., Fraver, S., Chen, G., 2018. Global pyrogenic carbon production during recent decades has created the potential for a large, Long-term sink of atmospheric CO2. J. Geophys. Res. Biogeosci. 123, 3682–3696. https://doi.org/10.1029/2018JG004490.

Zheng, Z., Zeng, Y., Li, S., Huang, W., 2016. A new burn severity index based on land surface temperature and enhanced vegetation index. Int. J. Appl. Earth Obs. Geoinf. 45, 84–94. https://doi.org/10.1016/j.jag.2015.11.002.